Investigations on the thermal calibration of sedimentary basin models – a case study from the Horn Graben in the Danish North Sea

Von der Fakultät für Georessourcen und Materialtechnik der

Rheinisch-Westfälischen Technischen Hochschule Aachen

zur Erlangung des akademischen Grades eines

Doktors der Naturwissenschaften

genehmigte Dissertation

vorgelegt von

Dipl.-Geol. Andreas Karl Anton Beha

aus Stuttgart

Berichter: Univ.-Prof. Dr.rer.nat. Ralf Littke
Univ.-Prof. Dr.rer.nat. Andreas Henk

Tag der mündlichen Prüfung: 30.November 2007

to my parents

Acknowledgements

I would like to take this opportunity to gratefully acknowledge those who have helped make this thesis possible. First of all, I would like to recognize my supervisors Professor Dr. Ralf Littke, head of the Institute of Geology and Geochemistry of Petroleum and Coal at Aachen University, and René Thomsen PhD, Director at Maersk Oil, for their continued support of my work. The many fruitful discussions with my supervisors lead to valuable contributions to this thesis.

I thank Professor Dr. Andreas Henk for his willingness to review this thesis.

The financial support provide by the German Research Foundation (DFG), which funded the first part of this work, is gratefully acknowledged. Without it, the initial research that yielded the groundwork of this thesis would not have been possible.

I would also like to recognize Maersk Oil, Denmark, for providing data and funding for the latter part of my research, which ultimately lead to the completion of this thesis.

Furthermore, I wish to thank all of my friends and co-workers at the Institute of Geology and Geochemistry of Petroleum and Coal at Aachen University for their friendship, discussions, and the myriad of other contributions that have not only lead to the completion of this thesis, but which made it a memorable experience. I also appreciate my co-workers at Maersk Oil, who helped to remind me that there is a life beyond researching for this thesis.

Special thanks go to Eva.

Abstract

The Horn Graben is a relatively under explored part of the Danish North Sea. Although extensive exploration in the adjacent Central Graben was very successful only three exploration wells have been drilled in the Danish part of the Horn Graben. Data obtained from two of the wells were used for calibration of 1D and 2D basin modelling studies conducted within the first part of this thesis. As the exploration wells did not find petroleum it was subject of the investigation to clarify why the wells were “dry” and where possible hydrocarbons are potentially trapped. Basin models in 2D or 3D were not yet carried out for the area investigated and only very few data exist from the subsurface in the Horn Graben. Especially the unproved Paleozoic source rock gives reason for numerous speculations. Basic information on the high probability of source rock deposits from this time are given by Nielsen et al. (1998) who showed Paleozoic sediments on top of crystalline basement on seismic images. Based on this work a deeply buried source rock was implemented in the 2D basin model. Properties of this sedimentary layer were interpolated from similar hydrocarbon sources in the adjacent German sector of the North Sea (Neunzert 1996). Remnants of the Upper Jurassic were assumed to contain source rock potential since comparable sediments in the Central Graben generated hydrocarbons during the past. However, the basin model showed that insufficient thermal stress on the Jurassic source prevented hydrocarbon transformation from kerogen. A different situation is observed for the Paleozoic source. Early to late maturity levels were calculated for this stratigraphic part of the graben. If the sediments are present, hydrocarbons must have been generated from this source since the Jurassic. Extensive salt deposits from the Permian most likely prevented secondary migration of hydrocarbons from the source rock to the reservoir rock. This is one possible explanation derived from the 2D basin model. A possible migration path perpendicular to the section strike can not be denied due to the 2D limitation of the model. The PetroMod modelling software still assumes that salt has complete sealing properties and prevents any kind of fluid from migrating into higher stratigraphic positions within the basin. Recently published work from Schoenherr et al. (2007) suggests that the sealing capacity of salt is limited and there are strong indications that the theory of salt acting as a complete seal needs to be revised. It is also very probable that thinning of the salt occurred in the area leading to “sweet spots” for vertical migration through the salt layer there.

During the calibration process of the Horn Graben wells questions arose regarding various limitations of the commonly used calibration method based on the EASY%Ro algorithm from Sweeney and Burnham (1990). By applying the pseudo-inverse method introduced by Thomsen and Noeth (2001) the models have been investigated regarding their resolution of the predicted maturity in the actual measured data points. Aiming at finding the simplest model that best matches the observed data led to revisions of heat flow histories initially applied and suggested for the 1D and 2D models in the first part of this thesis. Calculations for both wells led to different results for the “best fit” heat flow histories. The present day amount of heat flow was very similar in both wells whereas heat flow values calculated for the model start showed a greater difference. This can be explained with the purely mathematical approach of solving the problem.

The introduction of an “Instant Sensitivity Analysis Tool” in the third part of this work allows a very quick calibration of basin models to measured vitrinite data in the area investigated. Only a few model runs in the basin modelling software are necessary to obtain a “best fit” constant heat flow that best matches the observations. Additional to the “best fit” the tool allows finding uncertainty ranges very quickly. The quality of the predicted maturity trend compared to the measured data is expressed mathematically by the Mean Squared Residual (MSR), a unit-less expression of the goodness of fit. Results are reproducible and independent from individual and subjective basin modellers “best visual” outcome. For exploration purposes the precise quantification of “best fit” and “lower” and “upper” limits and its associated MSR help assessing risks and uncertainties.

Zusammenfassung

Der Horn Graben in der Dänischen Nordsee ist hinsichtlich der Kohlenwasserstoffexploration immer noch als relativ wenig untersuchtes Gebiet zu betrachten. Groß angelegte Explorationsprogramme im benachbarten Zentralgraben führten schon vor Jahrzehnten zu ergiebigen Erfolgen und bis zum heutigen Tag werden Kohlenwasserstoffe aus diesem Teil der Nordsee gefördert. Im dänischen Horn Graben wurden jedoch erst drei Explorationsbohrungen abgeteuft. Zwei davon lieferten die Datengrundlage zur Kalibrierung der 1D und 2D Beckensimulationsmodelle, die im Zuge dieser Arbeit erstellt wurden. In den erwähnten Bohrungen konnten keine Erdöl- oder Erdgasfunde gemacht werden, obwohl in beiden Fällen das angestrebte Reservoirgestein erreicht wurde. Dies gab Anlass zu untersuchen, was der Grund für fehlende Kohlenwasserstoffe in diesem Teil des Grabens sein könnte. Bisher wurden noch keine 2D oder 3D Beckensimulationsstudien über den Horn Graben angefertigt und veröffentlicht. Grund dafür könnte unter Anderem sein, dass nur sehr wenige Daten für dieses Gebiet existieren. Speziell die Präsenz eines potenziellen paläozoischen Muttergesteins konnte bisher nicht eindeutig nachgewiesen werden. Nielsen et al. (1998) zeigen jedoch Sedimente jener Zeit auf seismischen Schnitten. Aufgrund dieser Arbeit wurde im zweidimensionalen Beckenmodell ein heutzutage tief versenktes Muttergestein eingebaut. Eigenschaften wurden von vergleichbaren Sedimenten des Paläozoikums im benachbarten deutschen Gebiet übernommen (Neunzert 1996). Ein weiteres Muttergestein wurde in den verbleibenden Resten des Juras vermutet, da von

Gesteinen dieses Alters im Zentralgraben Kohlenwasserstoffe generiert wurden. Das Beckenmodell zeigte jedoch, dass die jurassischen Sedimente hinsichtlich ihres Potenzials zur Kohlenwasserstoffgenese noch als unreif bezeichnet werden müssen. Ein deutlich anderes Bild ergibt sich für die tief versenkten Gesteine aus dem Paläozoikum. Diese Einheit befindet sich theoretisch seit dem Jura in einem Reifefenster, das die Bildung von Kohlenwasserstoffen ermöglicht. Sollte das Muttergestein in diesem Teil des Grabens tatsächlich vorhanden sein, sind seit geraumer Zeit Kohlenwasserstoffe generiert worden. Vermutlich sind die Salzablagerungen des Perm Grund für eine verhinderte sekundäre Wanderung der Kohlenwasserstoffe vom Muttergestein zum Reservoir. Mögliche Migrationspfade senkrecht zum 2D Model können daher nicht gänzlich ausgeschlossen werden. Zudem wird in der Beckensimulationssoftware immer noch eine komplette Abdichtung durch Salzablagerungen angenommen. Neuere Arbeiten (Schoenherr et al. 2007) zeigen jedoch, dass die Annahme, Salz als impermeabel zu betrachten, überarbeitet werden muss. Es sollte weiter angenommen werden, dass eine lokale Ausdünnung der Salzablagerungen zu sogenannten „sweet spots“ geführt haben könnte, die Kohlenwasserstoffen einen Weg in stratigraphisch höher gelegene Einheiten ermöglicht haben könnten.

Während der Kalibrierung der Horn Graben Bohrungen und des 2D Schnitts ergaben sich Fragen hinsichtlich möglicher Einschränkungen der weithin gebräuchlichen Maturitätsberechnung nach Sweeney and Burnham (1990). Deshalb wurde die Auflösung des berechneten Maturitätstrends in den gemessenen Daten überprüft. Hierfür wurde die von Thomsen and Noeth

(2001) eingeführte pseudo-inverse Methode zur Berechnung der Güte des berechneten Maturitätstrends verglichen mit den gemessenen Daten verwendet. Ziel war es, die einfachste Wärmeflussgeschichte zu definieren, die zu einem höchstmöglichen Grad die gemessenen Daten reflektiert. Als Ergebnis mussten die im ersten Teil der Arbeit angenommenen Wärmeflussgeschichten teilweise revidiert werden. Die Wärmeflüsse, die ursprünglich für den heutigen Temperaturgradienten angenommen wurden, stimmen sehr gut mit den berechneten Werten überein. Größere Korrekturen mussten hingegen für den Anfang des Berechnungszeitraums durchgeführt werden. Die „best fit“ Wärmeflussgeschichten der beiden Bohrungen unterscheiden sich nun signifikant. Dies resultiert aus der rein mathematischen Herangehensweise und der bohrungsspezifischen Streuung der Maturitätsmesswerte.

Die Einführung des „Instant Sensitivty Analysis Tool“ (Hilfsmittel zur sofortigen Analyse der Sensitivität eines Parameters im Model) im dritten Teil der Arbeit ermöglicht das schnelle Abschätzen einer konstanten Wärmeflussgeschichte, wenn die thermische Geschichte eines Modells gegen Vitrinitreflexionswerte kalibriert wird. Nur wenige Modellrechnungen in der Beckensimulationssoftware sind nötig, um einen „best fit“ Wert zu finden, mit dem sich der Reifeparameter Vitrinitreflexion mit der bestmöglichen Genauigkeit modellieren lässt. Anschließende schnelle Abschätzungen des minimalen und des maximalen anzunehmenden Wärmeflussverlaufs helfen bei der Quantifizierung der Unsicherheit des untersuchten Parameters. Ständige Kontrolle über die Qualität der vorhergesagten Modellberechnungen ist durch die permanente Darstellung des Mean Squared Residual (MSR) gegeben. Diese Messgröße ohne physikalische Einheit zeigt die Abweichung der berechneten Werte gegenüber den gemessenen Daten an und ist deshalb ein direkter Indikator für die Genauigkeit der Kalkulation. Ein weiterer Vorteil der Methode sind objektive und reproduzierbare Ergebnisse. In der Exploration können die Resultate mit den dazugehörigen Fehlerabschätzungen direkt in die Bewertung von Prospekten eingehen.

Contents

1 Thesis overview

This thesis consists of three sections. Each section addresses different issues in basin modelling in general and thermal calibration against vitrinite reflectance data in particular. All sections contain case studies from the Horn Graben. Data available from this area allowed calculating models and comparing the results with real measured data. On this basis it was possible to verify theoretical assumptions described in the respective sections.

1.1 Section 2

The investigation of the thermal history and the hydrocarbon potential in the Horn Graben in the Danish North Sea was the initial focus of this thesis. No basin modelling study was published on this part of the Danish North Sea so far. Two exploration wells and one 2D seismic section perpendicular to the strike of the graben were used to model the thermal history and the hydrocarbon potential of the Horn Graben. Data from the two exploration wells were used to calibrate the thermal history of the models to measured data. Additionally the 2D model provided limited information on hydrocarbon migration. Previous work has been conducted on adjacent German graben systems by Rodon and Littke (2005) and Neunzert et al. (1996). Results from these studies helped to characterize the deeply buried Paleozoic sediments which are not yet drilled in the Horn Graben. Outcome of this section was a variety of possible heat flow histories that potentially controlled the thermal distribution in the graben. The different scenarios of course would have had a very different impact on thermal maturity evolution of the potential source rocks.

These observations led to the following questions: how good can we model the thermal maturity of sediments and what does the vitrinite reflectance data tell about thermal distribution and heat anomalies in the past?

1.2 Section 3

To answer the arisen questions a different approach was applied to the basin model in the third section of this thesis. Thomsen and Noeth (2001) introduced a pseudo-inverse method that allows finding the easiest heat flow history when calibrating against vitrinite reflectance data. With this method vitrinite reflectance trends versus depth are predicted based on a simple equation. Only a few model runs within the basin modelling software are necessary to map the results of this simple system into the complex. The method can help avoiding too many calculation steps on a trial and error basis for finding the “best fit” heat flow history. The instant calculation of the Mean Squared Residual (MSR) as a direct indicator of the misfit between the predicted and measured data provides a good possibility for monitoring the behaviour of the calculations. In the case of the Horn Graben a simple constant heat flow history did not fit all observed thermal indicators. When applying the “best fit” constant heat flow to the basin model the present day temperature gradient was too high compared to measured temperatures in the bore hole. Therefore a “best fit” present day heat flow was calculated separately using the pseudo inverse method. Subsequently a heat event in the past, reflected by a relatively high heat flow at the start of the model gradually declining to the present day value, was determined to fit the observed vitrinite data. The results from the third section of this thesis clearly showed that no additional complication in the heat flow history could better the fit between modelled and observed data.

1.3 Section 4

A tool for instant sensitivity analysis of predicted maturity trends in basin models compared to measured data is introduced in the fourth section of this thesis. The tool helps finding a “best fit” constant heat flow history when calibrating the basin model against vitrinite reflectance. Additionally an “upper” and “lower” acceptable range of the constant heat flow can be determined at the same time. Adequate parameter limits need to be defined in order to quantify the uncertainty of the heat flow history implied in the basin modelling study. At any point of the proposed workflow the basin modeller is in full control of the acceptable misfit of the three prediction trends compared to the measured data by the immediate calculation and display of the MSR. Basis for the “Instant Sensitivity Analysis Tool” is again the pseudo-inverse method by Thomsen and Noeth (2001). Main advantage of the tool is the reproducible determination of “best fit” heat flow histories independent from individual and very subjective “best visual fit” solutions for the predicted maturity of sediments in basin models.

2 Thermal history, hydrocarbon generation and migration in the Horn Graben in the Danish North Sea - a 2D basin modelling study

2.1 Abstract

In this study a 2D basin model has been built along a transect crossing the Horn Graben in WNW-ESE direction. The aim of the investigation was to improve the understanding of the thermal evolution of the basin and its influence on possible petroleum systems.

The 2D model of the subsurface is based on one seismic line and data from two exploration wells. Both wells TD'ed in Triassic sediments. The updoming of the Ringkøbing-Fyn High began during Late Carboniferous-Early Permian. At the end of the Permian the Horn Graben became active due to regional extension. The subsequent sedimentation history from Triassic to date is well recorded by well reports. A matter of debate has been whether or not significant amounts of Pre-Permian sediments exist in this area of the North Sea. Since organic material rich Paleozoic sediments serve as source rocks in widespread areas of North Germany and the southern North Sea it would be of great importance to know whether the same deposits exist in the Horn

Graben. Nielsen et al. (1998) introduced a model which shows Paleozoic sediments covering the basement at a maximum depth of 6.5 km. Assuming, Paleozoic sediments are underlying the Permian salt deposits there should be an active petroleum system present. The 2D model includes the Paleozoic source rock and tries to explain why two exploration wells have not found petroleum.

Key words Horn Graben • Danish North Sea • Basin modelling • Vitrinite reflectance • Petroleum Systems

2.2 Introduction

The aim of this study is to increase the general understanding of thermal history and hydrocarbon potential of the Horn Graben in the Danish North Sea. Numerical modelling of the thermal history and maturity was conducted on wells and pseudo wells in the late 1990s but is not published so far. Simulation of hydrocarbon generation from kerogen was not included in the former study and calibration of the 1D models was done solely against present day borehole temperatures and maturity data from regional wells in the German sector.

In this study two 1D models of exploration wells were constructed for calibration purposes and one 2D model was constructed for predictive and analysis purposes. Both wells are located directly on the seismic line, thus calibration of the 2D model was optimal. Vitrinite reflectance values have been measured from organic material rich sections of the wells. Therefore cutting material has been sampled and prepared.

As none of the wells was drilled deeper than Lower Triassic it was not possible to give evidence on whether or not a source rock is underlying the Zechstein salt.

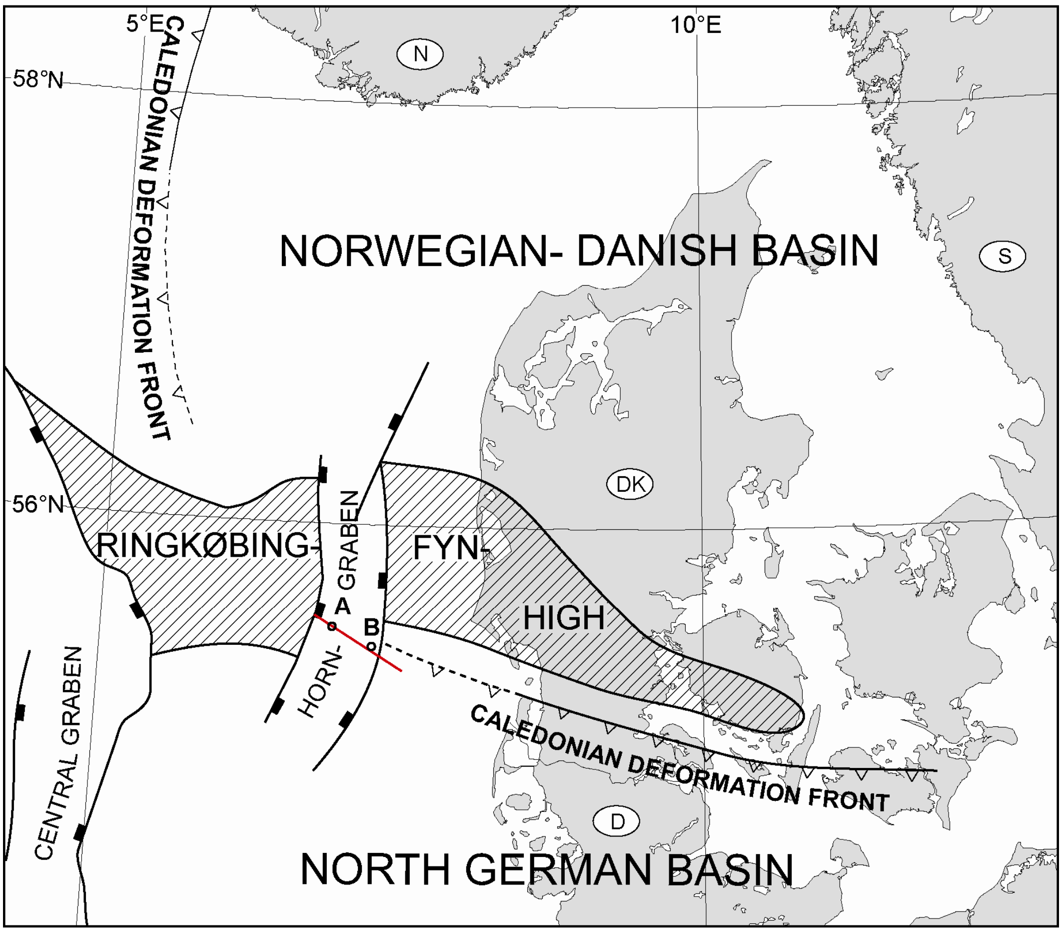

Figure 2.1: Geography of the study area and the adjacent major basin, graben and high structures.

The 2D model, however, includes the assumption that these Paleozoic sediments are present, buried up to a depth of 6500 meters. The assumption of presence of Paleozoic sediments is based on Nielsen et al. (1998), who interpreted Paleozoic sediments to be present on the Ringkøbing-Fyn High on seismic sections. Because the graben evolution took place during the period from Late Permian to Early Triassic times there is good reason to assume that deposition of Carboniferous sediments took place in what is at the present day the Horn Graben centre.

2.2.1 Database

For the 2D model discussed in this paper a WNW-ESE striking 2D seismic section perpendicular to the strike of the graben and two exploration wells were used. The wells are located directly on the seismic line and the stratigraphic levels found in the bore holes are tied to the seismic. By using the very detailed well reports good quality of the models was obtained.

Samples have been taken from both wells and vitrinite reflectance has been measured in order to establish the present thermal maturation of the sediments and reconstruct the thermal history of the area. Since the deposits from the Late Jurassic (Kimmeridgian) serve as a very good source rock in the Central Graben, these sediments were also regarded as potential source rocks for the Horn Graben. Additional to the maturation of vitrinite, Rock-Eval pyrolysis data and TOC measurements have been conducted from this stratigraphic level. These data were used for hydrocarbon modelling in the 2D part of this study. For estimation of the potential source rock properties within the Paleozoic sediments results from a former study in the Northwest German Basin (Neunzert et al. 1996) were adopted.

2.2.2 Study area

The Horn Graben is located between the Central Graben and the western coast of Denmark, some 50 to 100 km offshore in the North Sea (Fig. 2.1). It intersects the W-E striking Ringkøbing-Fyn High in NNE-SSW direction. The graben is divided into an eastward dipping halfgraben in the north and a westward dipping halfgraben in the south (Clausen and Korstgård 1994, Vejbæk 1990). The investigated area is situated in the southern part of the graben towards the German- Danish border.

2.3 Geological Background

The evolution of the Horn Graben initially started in the Late Permian - Early Triassic (Clausen and Korstgård 1993) when the main boundary fault on the western flank became active due to rifting. An east- west directed stress field during the Late Carboniferous- Early Permian (Ziegler 1990) led to crustal extension and thinning. Although evidence for volcanic processes can be seen in some parts of the Horn Graben, volcanic sediments are not present in the investigated area. The crystalline basement is not drilled and thus the only information is given by seismic and regional studies. Scheck et al. (2002) distinguishes between two basement types in this region. Northeast of the Caledonian Suture, Precambrian ages of 880-825 Ma prevail, whereas to the southwest, Caledonian ages of 450-415 Ma have been measured from metamorphic basement rocks. The study area is situated southwest of the suture and thus the basement has to be regarded as Caledonian gneiss (Best et al. 1983). Fig. 2.2 shows a sketch of the above lying sedimentary rocks and gives a short overview on the graben evolution.

Seismic data indicates faults in the basement which can be interpreted as syn-rift faults cutting into Paleozoic sediments and Zechstein. The graben shoulders are built by the East North Sea Block in the west and the West

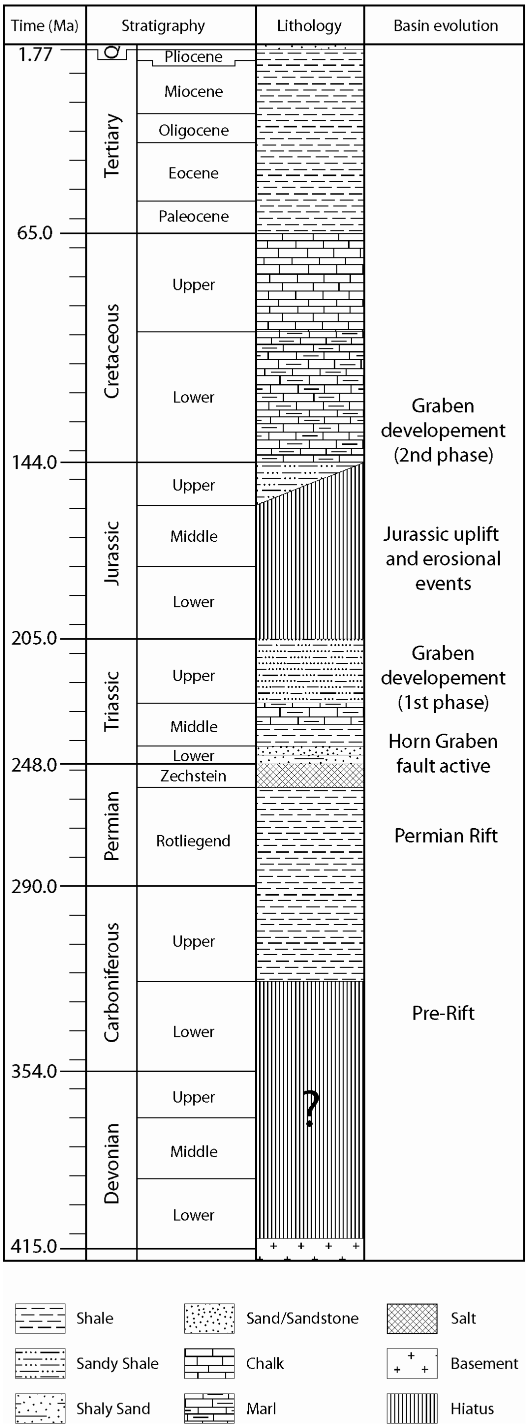

Figure 2.2: Regional stratigraphy in the study area.

Schleswig Block in the east (Rodon and Littke 2005). Both features are part of or directly linked to the Ringkøbing-Fyn High, an updomed area that was active from at least the Dinantian until the beginning of the Middle Oligocene (Best et al. 1983). This high separated the Northern from the Southern Permian basin. Both basins were filled with Rotliegend Sandstone from the Ringkøbing-Fyn High and Mid North Sea High, the London-Brabant Massif and Rhenish Massif in the south and from the Shetland Platform and the Fenno-Scandian High in the north (Ziegler 1990). Referring to Ziegler (1990) the investigated part of the Horn Graben was situated directly at the northern edge of the southern Permian basin and thus sediments in the Rotliegend section have to be regarded as fluvial deposits with land plant content. Relatively thick salt from the Late Permian covers both basins and also the Horn Graben the evolution of which began during that time. Early Triassic rifting took place without substantial mobilisation of Zechstein salt (Best et al. 1983) and led to rapid subsidence of the Horn Graben creating space for deposition of a huge amount of sediments. They originate mainly from the Fenno-Scandian High in the North (Ziegler 1990). Tectonically interesting is the evolution of a significant roll-over structure on the eastern flank of the Graben in the Lower and Middle Triassic. The development of a complex fault pattern due to collapse of sediments followed in the late Middle Triassic. Both deformations of the sediments play an important role in terms of trap formation as can be seen in the following chapters. In the Lower Jurassic approximately 250 m of claystone has been deposited and subsequently eroded in an uplift event during the Middle Jurassic (Bajocian- Bathonian) (Ziegler 1990, Michelsen 1989, Underhill and Partington 1993). The Late

Jurassic is characterised by sedimentation during Oxfordian to Early Tithonian. Remnants of these sediments are only found in the western part of the Graben. Another small uplift and erosion event took place in Late Tithonian time. From well reports one can see that all of the Upper Jurassic strata in the eastern part and approximately one third of those in the west have been eroded. Since Lower Cretaceous times until present the Horn Graben area underwent a relatively constant and undisturbed sedimentation.

2.4 Methods

2.4.1 Organic petrology and geochemistry

To estimate thermal maturity of sedimentary rocks the method of vitrinite reflectance measurement is commonly used. Vitrinite is a coalification product of humic substances, which originate from the lignin and cellulose of plant cell walls (Taylor et al. 1998). Vitrinite particles react on thermal stress with systematically increasing optical reflectance. This reaction is irreversible and therefore only the highest thermal imprint can be measured.

In this study 14 samples have been taken from every stratigraphic unit in both exploration wells. The standard procedure described by Taylor et al. (1998) was followed to conducting measurements.

The total organic carbon (TOC) content of the sediments has been measured to get information on the concentration of organic material in the potential source rock. For this purpose rock powder was burnt in a Leco RC 412 multi phase carbon analyser. At first the sample was heated from 350-520 °C at a rate of 2 °C/sec to detect the amount of organic carbon. In a second stage the temperature was increased from 520-1050 °C at a rate of 3 °C/sec to get the amount of inorganic carbon.

The measurements for Rock-Eval pyrolysis have been conducted following the workflow described by Espitalié et al. (1985).

2.4.2 Basin modelling

For simulation of realistic scenarios, the present day state, as interpreted from seismic, needs to be converted into numerical values. Thus geological, geophysical, geochemical and thermodynamic data are used to create a model that can be used to quantify processes at work during the formation of sedimentary basins. Forward modelling thus enables us to obtain results from different times during basin evolution and hydrocarbon transformation. Basic work on basin modelling was done and published by Yükler et al. (1978), Nakayama and Van Siclen (1981), Welte and Yükler (1981), Bethke (1985), Nakayama and Lerche (1987), Welte and Yalcin (1987), Lerche (1990a, b), Thomsen (1994) and Welte et al. (1997).

In this study all models were generated with the PetroMod suite of modelling software from IES GmbH, Germany. Initially 1D conceptual models were put together for the two exploration wells based on the observed geological, geochemical and geophysical data brought into a temporal framework. The history of the basin was then subdivided into discrete time steps or events.

Potential events are those of deposition, erosion and non-deposition (hiatus) defined by a specific start- and end-point in time. Afterwards the discretised model of the basin history is translated into a numerical form that describes the physical and temporal properties, which can be read by the basin simulator. The conceptual model of this study is based on well reports, the

Event no	Event name	Age at base [Ma]	Thickness [m]	Lithology	SWI [°C]	HF [mW/m^2]
28	Quaternary	1.77	250	SANDsilty	5.0	52
27	Tertiary	65	594	SHALE	22.7	53
26	Upper Cretaceous	98.9	456	CHALK	25.9	54
25	Upper Albian I	103	32	SHALE	26.3	54
24	Upper Albian II	106	25	LIMESTONE	26.4	55
23	Lower Albian HIATUS	112.2	0	None	26.5	56
22	Upper Aptian HIATUS	116	0	None	26.6	56
21	Lower Aptian	121	6	MARL	26.6	56
20	Upper Barremian HIATUS	124	0	None	26.4	56
19	Lower Barremian	127	36	MARL	26.2	56
18	Upper Hauterivian	129.5	43	SHALEcalc	26.0	56
17	Lower Hauterivian HIATUS	132	0	None	25.8	56
16	Valanginian	137	69	SHALE	25.4	56
15	Berriasian HIATUS	144.2	0	None	25.0	57
14	Upper Jurassic EROSION	150.7	-120	None	24.7	57
13	Upper Jurassic	159.4	120	SHALEsilt	23.3	58
12	Lower Jurassic EROSION	180.1	-250	None	23.1	60
11	Lower Jurassic	205.7	250	SHALE	22.2	64
10	Ladinian/Keuper	234.3	648	SHALEsilt	25.0	79
9	Anisian	241.7	44	LIMEcarbo	24.5	87
8	Olenekian	244.8	330	LIMEdolom	24.5	91
7	Induan I	245.3	140	SHALE	24.6	91
6	Induan II Upper Pele	245.5	34	SANDSTONE	24.6	91
5	Induan III	246	375	SHALEsilt	24.6	92
4	Induan IV Lower Pele	246.6	193	SANDsilty	24.3	93
3	Induan V	247.1	83	SILTshaly	24.1	94
2	Induan VI Volpriehausen	247.7	100	SANDsilty	24.1	94
1	Induan VII Bunter Shale	248.2	41	SILTshaly	24.1	95

Table 2.1: Input data for modelling of burial, erosion and temperature history of well B (for physical rock properties see Table 2).

seismic section and general information of the basin evolution given by Best et al. (1983), Underhill and Partington (1993) and Ziegler (1990). For the chronostratigraphic subdivision time scales of Gradstein et al. (1994) for the

Mesozoic and Berggren et al. (1995) for the Cenozoic were used. Time information of the Paleozoic was given by the time scale of the Geological Society of America (1999)
(http://www.geosociety.org/sience/timescale/timescl.htm).

Because of the fact that organic material reacts on increasing thermal stress, a critical parameter for the basin evolution and the hydrocarbon transformation is the temperature history. Thus the simulator needs to calculate the thermal condition for every time step of the model. For calculation of vitrinite reflectance from temperature histories, the EASY%Ro algorithm of Sweeney and Burnham (1990) was used. With this model vitrinite reflectance values between 0.3 and 4.5% VR_r can be calculated. To calibrate the burial and thermal history plots of the measured vitrinite reflectance and temperature data points against the calculated trend lines are used.

For the 1D modelling the input dataset for well B is shown in Table 2.1. Thickness, lithology, age, sediment/water interface temperature and basal heat flow values are listed for every stratigraphic unit. The sedimentary rock properties are of great importance for calculation of the maturation. Besides burial depth, basal heat flow and sediment/water interface temperature as outer boundary conditions, radioactive heat production, heat conductivity and heat capacity of the different rock types have an impact on the thermal evolution. These rock specific parameters of the applied lithologies in the models are summarized in Table 2.2.

Lithology	Density [kg/m^3]	Compressibility [1/Pa]		Thermal Conductivity [W/mK]		Heat Capacity [cal/gK]	
		Minimum	Maximum	20°	100°	20°	100°
SHALE	2,680	10	60,000	1.98	1.91	0.213	0.258
SHALEsilt	2,677	10	25,000	2.05	1.94	0.210	0.254
SHALEcalc	2,688	10	5,000	2.22	2.09	0.208	0.248
SHALEsand	2,674	10	9,000	2.32	2.12	0.205	0.248
LIMESTONE	2,710	10	150	2.83	2.56	0.195	0.223
LIMEdolom	2,752	10	180	3.18	2.82	0.198	0.226
LIMEshaly	2,700	10	550	2.51	2.31	0.203	0.237
LIMEcarbo	2,696	25	420	2.37	2.13	0.195	0.225
MARL	2,687	10	940	2.23	2.11	0.208	0.248
CHALK	2,700	45	700	2.85	2.51	0.197	0.226
SILTshaly	2,675	10	15,000	2.09	1.98	0.203	0.245
SANDSTONE	2,660	10	500	3.12	2.64	0.178	0.209
SANDsilty	2,664	10	1,200	2.97	2.64	0.188	0.223
SALT	2,160	1	4	5.69	4.76	0.206	0.212
BASEMENT	2,750	1	2	2.72	2.35	0.188	0.223

Table 2.2: Petrophysical parameters of the sedimentary rocks and the basement used in basin modelling.

2.5 Results and discussion

2.5.1 Vitrinite reflectance data

A total of 14 samples, 7 for each of the two exploration wells, have been taken from cutting material. Only 1 sample did not contain enough vitrinite particles to obtain reasonable results. The remaining samples show a characteristic pattern of thermal maturity for nearly the entire stratigraphy range from Middle Triassic to Tertiary. Results of the measurements are listed in Table 2.3.

Well	Stratigraphic unit	Depth [m]	VR_r [%]	n	SD
A	Tertiary	895	0.23	50	0.03
A	Upper Jurassic	1550	0.41	33	0.07
A	Olenekian	2572	0.63	23	0.06
A	Induan III	3017	0.73	27	0.1
A	Lower Pele	3438	0.79	15	0.05
A	Volpriehausen	3660	0.92	15	0.09
B	Tertiary	440	0.2	38	0.08
B	Tertiary	792	0.23	50	0.05
B	Upper Cretaceous	1158	0.24	28	0.04
B	Ladinian/Keuper	1600	0.43	13	0.07
B	Ladinian/Keuper	1978	0.59	4	0.11
B	Induan I	2610	0.73	6	0.15
B	Volpriehausen	3430	0.88	14	0.08

Table 2.3: Vitrinite reflectance data. n is the number of measurements at the respective depth, SD is the standard deviation.

2.5.2 TOC and Rock-Eval pyrolysis data

TOC and Rock-Eval pyrolysis measurements were conducted to get information on quantity and quality of organic matter. This information is used for calculation of generated hydrocarbons that have been transformed from organic matter in the source rocks. Both exploration wells end in Triassic sediments and thus TOC and Rock-Eval pyrolysis data on the most important source rocks, the Paleozoic deposits, could not be measured. The Upper Jurassic source rock was only drilled by well A. For this stratigraphic unit a TOC content of 1.5% was measured. The Rock-Eval pyrolysis showed values of 0.3 mg/g rock for the S1 peak, 2.75 mg/g rock for the S2 peak and 2.07 mg/g rock for the S3 peak. From this data a Hydrogen Index (HI) of 183 was calculated by the formula: HI= (100 x S2)/TOC. The T_{max} value is at 428 °C, i.e. in the immature range.

2.5.3 1D numerical modelling: conceptual model and burial history

Two exploration wells provided the base information for the 1D models. The results from the 1D modelling give an overview of temperature and burial history in this particular part of the Horn Graben. The conceptual models are based on the geological evolution described in the 'geological background' section of this publication. As a first step the different stratigraphy levels from both well reports were put into PetroMod 1D. The deepest drilled sediments are of Induan (Early Triassic) time. As the graben evolution led to formation of huge accommodation space for deposition, up to 1100 m of sediments have been deposited in the graben centre in less than 3 million years (Fig. 2.3). Mainly shale and silty shale dominate the Induan lithology. However, of greater interest are the potential reservoirs Volpriehausen equivalent and Lower and Upper Pele sandstone equivalent represented by 33 to 230 m thick sandstone layers that are recognized within this section. Because of their structural position and their still very high porosity these sands were targeted by the exploration wells. During the Olenekian and Anisian a series of mainly limestones covered the older sediments. A silty shale of Ladinian/Keuper age builds the top of the Triassic section. From Early to Late Jurassic the investigated area underwent phases of deposition with subsequent erosion. Ziegler (1990) estimates some 250 meters of deposits for the Lower Jurassic mainly consisting of claystone (Michelsen 1989), which were eroded during the Middle Jurassic due to Cimmerian thermal uplift and exposition of the rocks (Andsbjerg et al. 2001, Nielsen 2003). For the Upper Jurassic an asymmetric nature with regards to the presence of sediments from this time is seen in the graben.

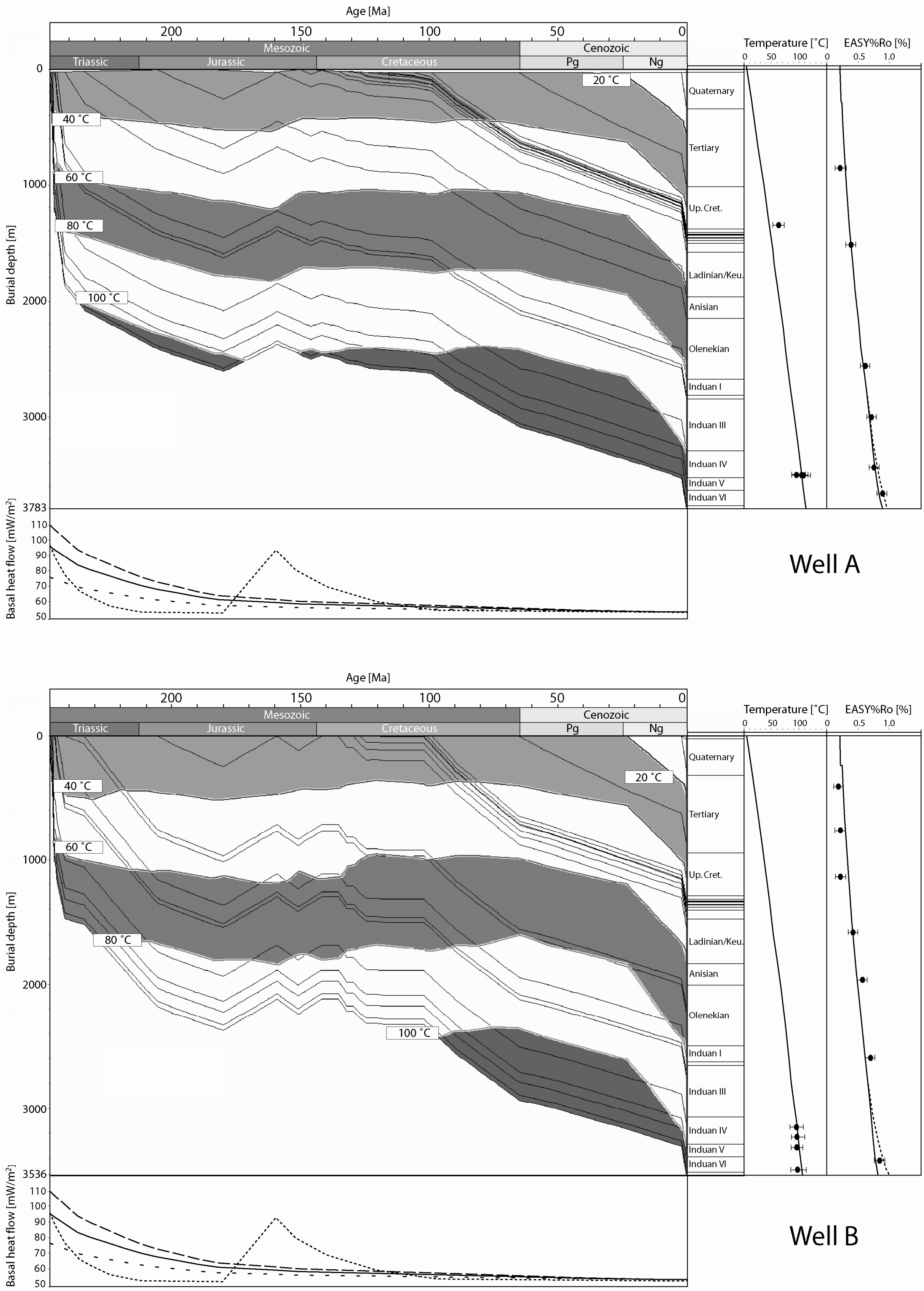

Figure 2.3: Burial, heat flow and temperature histories. Measured (dots) and calculated (lines) temperature and vitrinite data for well A and well B.

After Ziegler (1990) approximately 140 meters of sandy shale have been deposited during the Late Jurassic. A Late Cimmerian phase led to erosion in the Late Jurassic to Early Cretaceous. Thus none of these sediments were encountered in well B. The record of sediments in well A shows that only one third of the amount of Upper Jurassic strata has been eroded in this part of the graben (Fig. 2.3). The Lower Cretaceous is marked by sedimentation of 120 meters of dominantly marls and shales. Several hiati are seen in the sedimentary records of the wells. With 370 m a relatively thick layer of chalk has been deposited during the Upper Cretaceous. Constant sedimentation took place during Tertiary and Quaternary times when shale and silty sand completed the stratigraphic succession of both wells.

2.5.4 1D numerical modelling: thermal and maturity history

The most important parameters for thermal and maturity history modelling are basal heat flow and the burial history. Since well reports from both exploration wells give very good information on stratigraphy, the Post-Permian burial history of the 1D models was relatively easy to reconstruct. The reconstruction of the heat flow history was done using measured vitrinite reflectance assuming that vitrinite reflectance can be adequately calculated using the EASY%Ro algorithm (Sweeney and Burnham 1990). The calibration of the model leads to a depth/vitrinite reflectance plot that compares measured with calculated data. In Fig. 2.3 the palaeo heat flow and the temperature and maturity calibration data are added to the burial history plot of both wells.

The present day basal heat flow is calibrated using measured temperatures in the wells. In both wells 52 mW/m^2 gives a very good match for the temperature field. For reconstruction of the heat flow history from the beginning of basin formation until Miocene two different scenarios have been applied to the 1D models. One assumes only a heat flow maximum at the model start with a typical value of 95 mW/m^2 for this kind of burial history of a post rift basin. A second heat flow history includes an additional heat event due to the Jurassic doming. Stretching factors (β) have been calculated for both rift events. Approximately 1.9 for the initial rift event and approximately 1.3 for the Jurassic rift match the time span and amount of subsidence for each of the rifting stages. Consequently a heat flow history with a maximum heat flow of 95 mW/m^2 at the model start declining to 52 mW/m^2 at 180 Ma before present and a second maximum of 92 mW/m^2 occurring at 160 Ma and declining to a present day value of 52 mW/m^2 was used according to McKenzie (1978). A sensitivity study for heat flow variations showed that the model reacts very insensitive on heat flow variations during the past. The sensitivity analysis also shows that the present day maturity pattern is mainly controlled by Neogene heat flux and subsidence. Both, the applied heat flow histories and the calculated results are shown in Fig. 2.3. The impact of the two different heat flow variations on the petroleum systems and the maturation and alteration of kerogen will be discussed in the 2D modelling part of this study.

The thermal and maturity evolution based on the assumed heat flow history and the burial history of the sedimentary rocks shows rapid increase of temperature and maturity at the beginning of the graben formation. Already in

Lower to Middle Triassic time the deepest buried sediments reach high maturity levels in relatively short time. The temperature curve shows the same sensitivity to the graben evolution. The strongest increase of temperature occurred in the Early Triassic due to rapid burial of the sediments. Only minor increase in temperature has occurred since Olenekian.

2.5.5 2D numerical modelling: model construction and parameters

A 2D model based on a seismic section perpendicular to the strike direction of the Horn Graben was constructed. The 2D section has a NNW-SSE orientation and a length of about 57 km. Both exploration wells are directly located on the section; well A about 13 km and well B about 36 km from the western boundary of the model. The interpreted seismic section together with the two exploration wells were used to construct the 2D geometries for the PetroMod model. Results with respect to heat flow and burial history from 1D modelling have been used to constrain the model boundary conditions. Fig. 2.4 shows the model geometry, faults and well locations.

The 2D section was extended in depth compared to the models from the 1D part of the study by interpreting three additional layers on the seismic section. Thus Zechstein salt and the assumed Paleozoic sediments complete the model geometry, underlain by the basement. The deepest burial of sediments is now at a maximum depth of 6500 meters. The 2D model event history consists of 18 layers at present day, plus two erosion events during the

Jurassic. Table 2.4 shows the lithologies, deposition and erosion ages of the different layers.

Event	Event name	Age at base [Ma]	Lithology	SWI [°C]	HF [mW/m2]
21	Quaternary	1.77	SANDsilty	7.0	52
20	Tertiary	65	SHALE	21.7	54
19	Upper Cretaceous	98.9	CHALK	25.0	55
18	Lower Cretaceous	144.2	MARL	23.6	57
17	Upper Jurassic EROSION	150.7	None	23.3	57
16	Upper Jurassic	159.4	SHALE	22.4	58
15	Lower Jurassic EROSION	180.1	None	20.0	60
14	Lower Jurassic	205.7	SHALE	21.8	64
13	Ladinian/Keuper	234.3	SHALEsilt	26.2	80
12	Anisian	241.7	LIMEcarbo	26.4	87
11	Olenekian	244.8	LIMEshaly	26.1	91
10	Induan I	245.3	SHALE	26.0	91
9	Upper Pele Sand	245.5	SANDSTONE	26.0	91
8	Induan III	246	SHALEsilt	25.9	92
7	Lower Pele Sand	246.6	SANDsilty	25.9	93
6	Induan V	247.1	SILTshaly	25.7	94
5	Volpriehausen Sand	247.7	SANDsilty	25.5	94
4	Induan VII	248.2	SILTshaly	25.5	95
3	Salt	256	SALT	25.0	60
2	Paleozoic Sediments	323	SHALE	25.0	60
1	Basement	415	BASEMENT	no value	60

Table 2.4: Input data for modelling of burial, erosion and temperature history of the 2D section. (for petrophysical properties of the sedimentary rocks see Table 2.2).

The faults recognized on the seismic data were also included in the 2D model and their influence on migration investigated. Since no information on fault properties was available, two models have been run with the extreme cases: one model kept all faults open through time the other estimated sealed faults.

In the 2D model hydrocarbon generation and migration are investigated by introducing two source rock layers in the model. An Upper Jurassic source rock for which cutting samples were available was modelled as a type II source rock with a measured TOC value of 1.52% and a hydrogen index (HI) of 183. The reaction kinetics was adopted from Pepper and Corvi (1995). A second Upper Carboniferous and Lower Permian source rock was modelled as a combined homogeneous section. The Lower Permian which is represented by sandstone deposits in the northern and southern Permian basin can not be regarded as a possible reservoir rock in this section because this part of the Horn Graben was situated at the northern margin of the southern Permian basin. Thus for the model it was assumed that there were no significant amounts of sediments accumulated during this time. Source rock parameters for the Paleozoic were extrapolated from the Northwest German basin since they were not drilled in the investigated area. Neunzert et al. (1996) reports values of up to 1.19% TOC and a HI of up to 59 and interpreted samples from these sediments as kerogen Type III. Thus the reaction kinetics presented by Pepper and Corvi (1995) for type III source rocks were applied.

Reservoir and seal layers did not have to be defined in the model since these properties only depend on calculated porosity and permeability. Predicted for these features were the sandstone intervals from the Triassic as reservoirs and the overlying capping shales from the same stratigraphic section as seals. Based on the tectonic evolution of the graben, two structural hydrocarbon traps could have formed, one on each side of the graben boundaries.

The objectives of the 2D modelling part of the study were to answer the following questions:

1.) Does the thermal and maturity history from 1D modelling match the 2D situation?
2.) Which possible processes can be responsible for not having hydrocarbon accumulations in the potential structural traps?

2.5.6 2D numerical modelling: structural evolution

The initial stage of the structural evolution of the graben was a regional stretching event leading to the opening of the basin at Late Permian to Early Triassic times. Every following event described in the chapter 'Geological background' is represented in the 2D model.

The structural evolution of the graben was not in the focus of this study, but relevant events for hydrocarbon migration and trapping have been investigated. For a detailed structural analysis of the Horn Graben see Best et al. (1983).

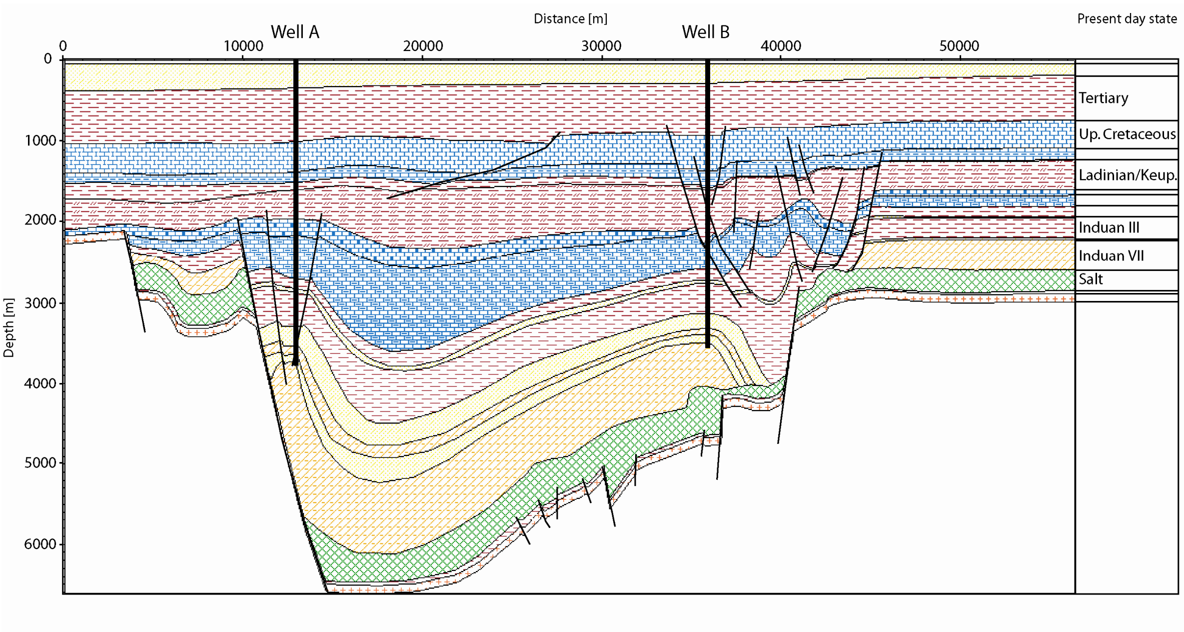

Figure 2.4: 2D model geometry with well locations.

The main features for hydrocarbon trapping are the structural highs (Fig. 2.4) which developed in the course of major subsidence of the graben centre. As a result deformation of the potential reservoir sandstones occurred on the western boundary and the development of a roll-over structure on the eastern margin of the central Horn Graben. Both structures are sealed by intraformational shales. Also a syn-sedimentary collapse structure above the eastern boundary fault with its sandstone layers sealed by a complex fault pattern could be regarded as a potential reservoir structure.

Salt movements were not modelled since no evidence for salt mobility in this part of the graben is given by the seismic data. This conclusion is supported by Clausen and Korstgård (1996). Thus no salt diapirs with associated reservoir potential in the rim synclines are present.

Nevertheless the salt plays an important role not only in terms of temperature distribution but also in terms of hydrocarbon migration since it seems to cover and seal the complete centre of the graben.

2.5.7 2D numerical modelling: thermal and maturity evolution

The 2D model was calibrated by comparing the measured vitrinite reflectance data from sediment samples taken from the exploration wells with calculated data. As expected applying the heat flow histories reconstructed by 1D modelling for the entire 2D section resulted in a very good match between measured and calculated maturity and present day temperature data. Fig. 2.5 shows the maturation pattern for the Horn Graben.

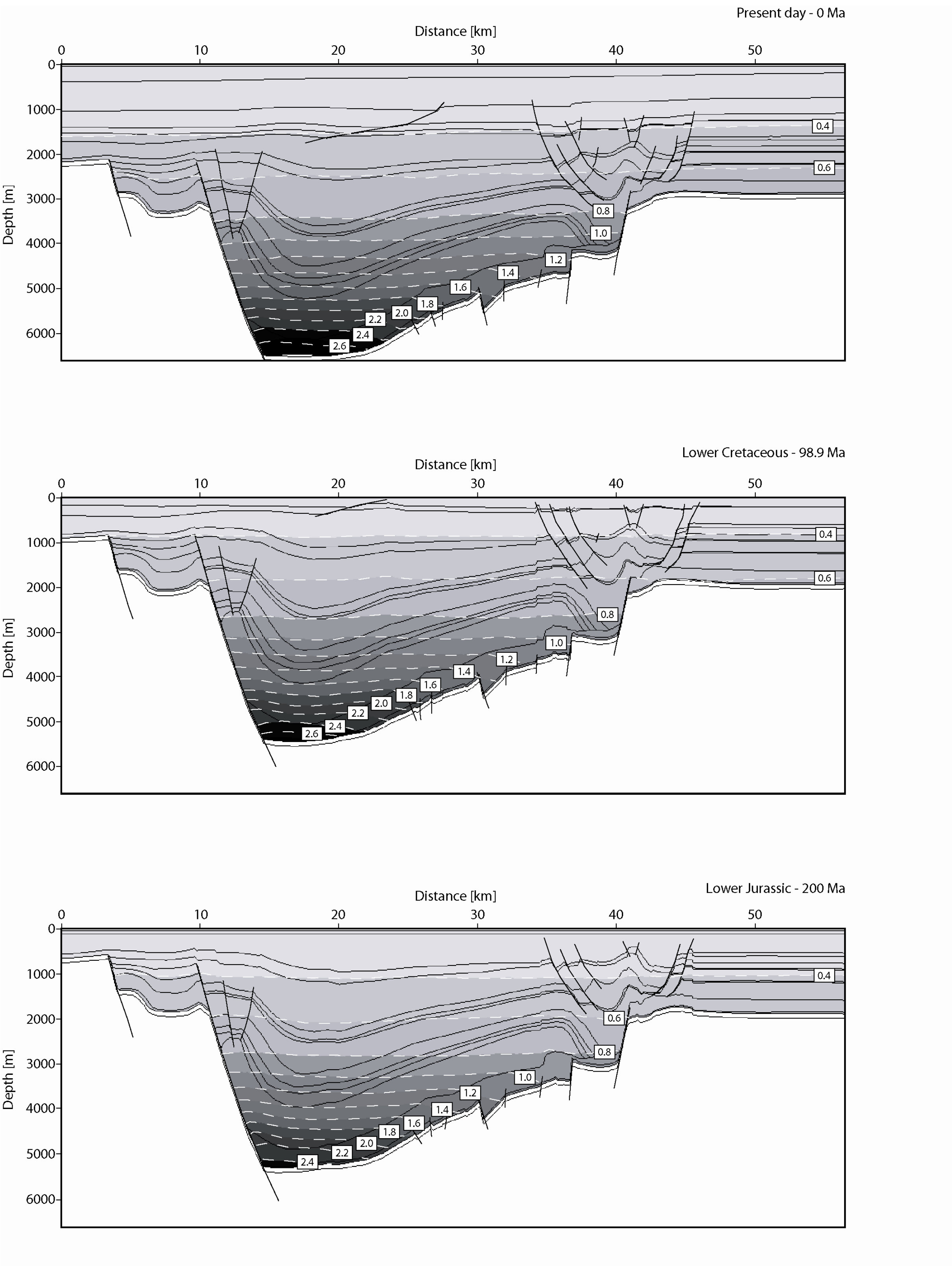

Figure 2.5: Maturity pattern of the sediments for three events. Lower Jurassic (200 Ma), Lower Cretaceous (98.9 Ma) and Present day.

The interesting sections of the model in terms of hydrocarbon formation are the Upper Jurassic and the deeply buried Paleozoic deposits. Since Late Triassic times the rapid subsidence decelerated and only few sediments accumulated on top of the whole section. At present day the Upper Jurassic maximum burial is at a depth of approximately 1700 meters. Due to its shallow position in the sedimentary stack and the comparably low heat flow values over time, thermal maturation of these sediments is not high enough to transform organic material into hydrocarbons. The immature stage of the Upper Jurassic is supported by measured vitrinite reflectance data (0.41% VR_r). In order to reach the early oil window this layer should have been buried at least 500 meters deeper.

A different situation can be deduced for the deep Paleozoic source rocks. At present day the sediments are situated in the “early to late oil generation window” (0.55-0.7% VR_r and 0.7-1.3% VR_r) on the graben shoulders at a depth of 2800 to 3200 meters. In the graben centre the Paleozoic reaches maturity levels from “wet gas” to “dry gas” (1.3-2.0% VR_r and 2.0-4.0% VR_r) at burial depths from 4100 to 6500 meters.

For exploration purposes it is of great interest to study how transformation of the deepest buried organic material evolved through time. Therefore two modelled grid cells shown in Figure 2.6 were chosen to study temperature and maturation evolution through time. The first cell 5408 is located in the western central part of the graben. In both heat flow variants transformation from kerogen to hydrocarbon started in Early to Middle Triassic times about 246 million years before present.

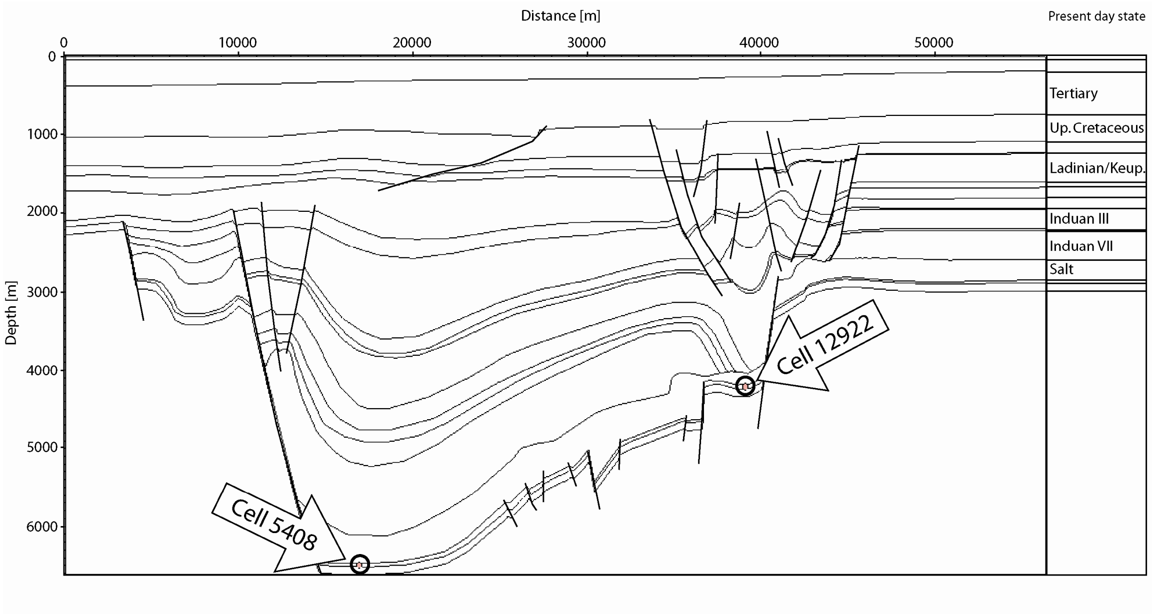

Figure 2.6: Location of the cells which are examples for the different maturation of the same sedimentary unit in the Horn Graben. Cell 5408 is located in the deepest part of the graben, cell 12922 shows the evolution of shallower buried Paleozoic sediments at the graben center margin.

Depending on which of the two heat flow histories is applied to the 2D model a slightly different pattern of temperature and maturity development and transformation ratio and bulk generation is seen in Fig. 2.7. In both cases, however, the Early Triassic has the most obvious impact on sediments. The maturity of the deeply buried sediments further increases due to the second heat anomaly during the Jurassic heat event when the heat flow history with two heat anomalies is applied to the model. However, this does not have a big impact on the transformation ratio of the kerogen since most of it has already been transformed by this time. Both models end with total transformation of kerogen into hydrocarbons at present day.

For the Paleozoic at the eastern rim of the graben centre a different transformation history is found. There, cell 12922 shows a different evolution. The burial depth of these sediments is shallow compared to the western graben centre and the peak of hydrocarbon generation is estimated to have occurred only about 160 million years before present when the Jurassic heat event affects this part of the graben. In case of only one heat anomaly at model start no clear peak of hydrocarbon transformation is shown. The results also show that only 60% of the organic material is consumed at present in both cases. According to the kinetics hydrocarbons generated in the eastern part of the graben centre would consist mainly of oil since burial of sediments at the eastern graben boundary only touches the wet gas window. However, oil is generally not expelled from coaly source rocks like those present in the Carboniferous of central-western Europe, but kept in the source rock until cracking to gas occurs at higher temperatures (Littke and Leythaeuser, 1993). Fig. 2.7 shows the comparison of the temperature, thermal maturity, transformation ratio and bulk generation rate history for Paleozoic source rocks in the western and eastern graben centre. Two important questions arise concerning the model results and the present day situation:

1) Where are the hydrocarbons generated extensively from the Paleozoic deposits?
2) Why did they not fill the expected reservoirs?

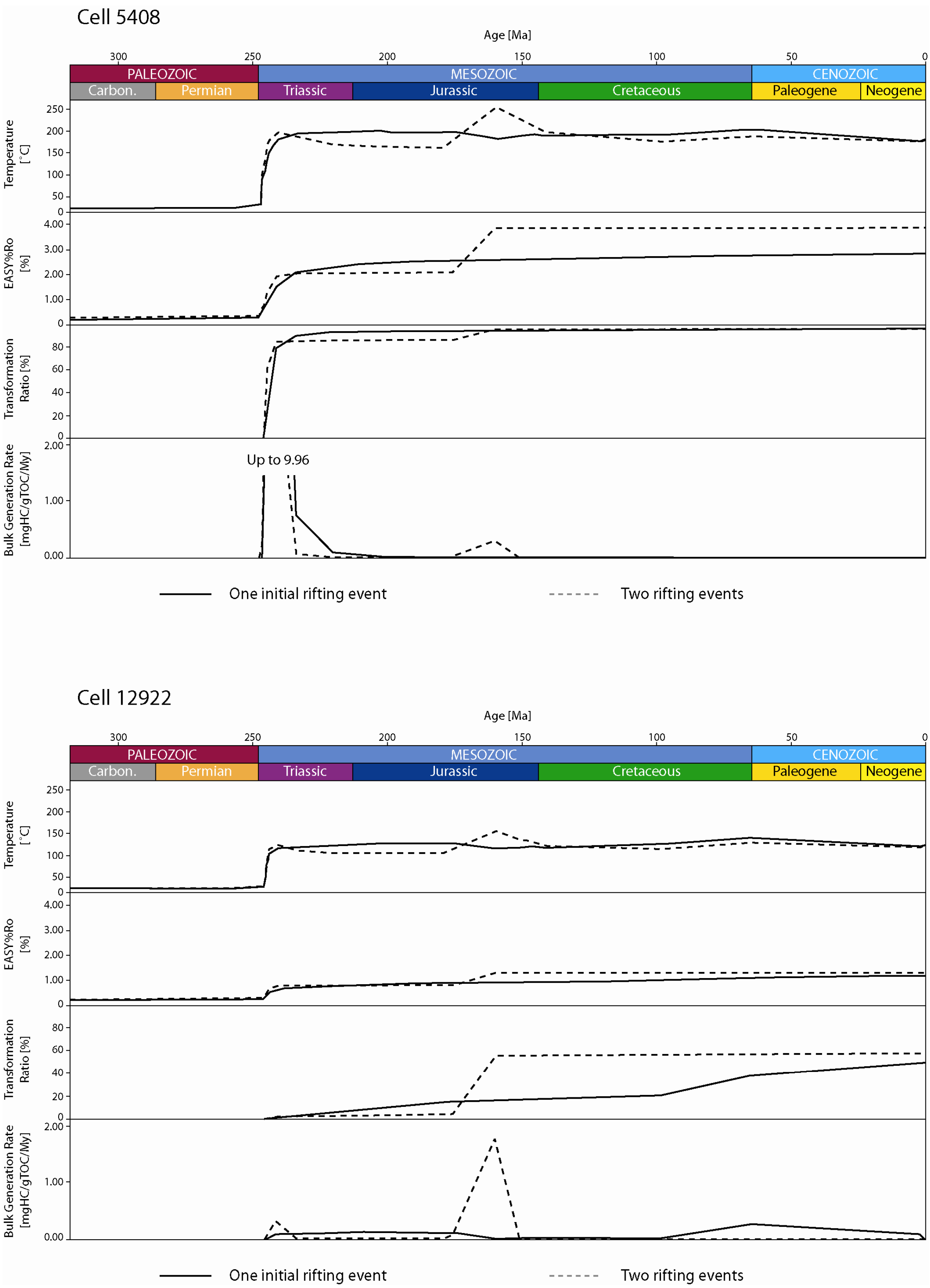

Figure 2.7: Comparison of the temperature, maturity and transformation ratio history for cell 5408, a modelled fragment of the Paleozoic sediments from the deepest part of the graben centre with cell 12922 from shallower buried eastern part of the graben.

2.5.8 2D numerical modelling: hydrocarbon migration

Under the assumption that the modelled source rock of Late Paleozoic age is present, thermal maturity and burial history should have led to hydrocarbon formation. The hydrocarbons must have accumulated somewhere or disappeared through time. As a result from modelling it is obvious that hydrocarbon migration only took place within the source rock level. No secondary migration into higher stratigraphic levels is possible due to salt sealing and lack of faults cutting the salt. Due to the 2D limitation in space, no statement on flow paths perpendicular to the modelled section, which could be a possible way for hydrocarbons out of the source, can be set.

In the 2D model, even assignment of more open fault properties did not result in secondary migration into the reservoirs. This is due to the impermeable nature of the salt, leading to perfect sealing conditions. It is, however, very probable that thinning of the salt occurs in the area leading to “sweet spots” for vertical migration through the salt layer there. These might be possible targets for future exploration in the Horn Graben. Furthermore, it should be noted that migration of petroleum in salt is known to occur as recently reported (Schoenherr et al., 2007).

2.6 Conclusions

One goal of this study was to clarify why no oil and gas was found in the targeted reservoirs. Source rock presence and its properties within the graben was high risk from the beginning of exploration. The Upper Jurassic (Kimmeridgian) source has been drilled and geochemical analyses have been conducted. As a result from the 2D modelling the Upper Jurassic source must be regarded as immature, with the consequence that no hydrocarbons were generated from kerogen in this stratigraphic level. For the model the presence of a deeply buried Paleozoic sedimentary unit with source rock properties was assumed. Since there were no measured data available extrapolation data from the adjacent German sector of the North Sea helped to create a model with reasonable TOC and HI values for this stratigraphic unit. The assumed Paleozoic source rock was buried to a depth which easily allows generation of hydrocarbons. The reason for not accumulating hydrocarbons in the reservoirs although traps are present is the impossible ‘secondary migration’ from the source rock towards the reservoir rocks. The model shows only ‘primary migration’ within the source rock since Early Triassic times, as the Permian Zechstein salt which seals the Paleozoic does not allow any further migration. A possible migration pathway could be provided by the faults. Models with different fault properties were created to investigate this issue. Since there was no reliable information about the faults, we decided to simulate the two extreme cases. One model kept all faults ‘closed’ and one model used more ‘open’ fault properties. Both fault characteristics were set constant for the entire history of the graben. No secondary hydrocarbon migration from source to reservoir occurred in any of the cases.

Concluding two possible reasons can be drawn for the fact that no hydrocarbon accumulations can be found in the reservoirs of this particular part of the Horn Graben:

a) The assumed deep buried Paleozoic source is not present in this part of the graben.

b) The Zechstein salt serves as highly impermeable seal and prevents generated hydrocarbons from migrating into higher stratigraphic levels.

3 A quick method to quantify resolution limits of heat flow estimates in basin models.

3.1 Abstract

Deterministic forward basin models are generally used to quantify processes at work during basin evolution. This article describes a work flow for quick calibration of palaeo heat flow behavior by determining a heat flow history that best matches observed data, such as vitrinite reflectance, used as indicators for the thermal maturation of sediments. A limiting factor for determining heat flow history is the ability of the algorithm used in the software for maturity calculation to resolve information inherent in the data used for calibration. Thermal maturation is controlled by the temperature field in the basin through time and thus greatly affected by maximum burial depth of the sedimentary units. Calibration, or finding the thermal history model that best fits observed data (temperature and thermal indicators such as vitrinite reflectance) is often a very time consuming exercise. To shorten this process a simple pseudo-inverse model based on inverse methods suggested by Lerche (1991) and

introduced by Thomsen and Noeth (2001) is used to map a complex thermal behaviour obtained in a basin simulator into a simple behaviour using a simple equation. By comparing the calculated “simple” maturation trend with the observed data points using the suggested workflow it becomes trivial to evaluate the range within which a best fit model will most likely be found. Consequent reverse mapping from the simple model to the complex behaviour results in precise values for the heat flow that can subsequently be applied for the basin model. Two case studies have been conducted on wells in the Horn Graben in the Danish North Sea, where calibrating the model using a constant heat flow through the basin history is not justified. A more complex thermal history must be considered and the pseudo-inverse method therefore has been applied in a sequence of refining steps to investigate more complex heat flow history behaviours. Neither in the observed maturity data nor in the recorded stratigraphy is there evidence for extensive erosion which would have influenced the thermal maturity pattern seen at present day. Thus only the variations of heat flow and time parameters were subject of the investigation. The aim of the work flow is to determine the simplest “best fit” heat flow history according to the maximum resolution given by the measured maturity data.

3.2 Introduction

Basin modelling is commonly used in quantitative petroleum studies. At the beginning of every modelling project calibration of various input parameters valid in the specific region of interest is important. Lithology linked to the stratigraphic unit, calibration data and thermal history are basic information for the numerical model and the resulting model is only as good as the calculated results match the observed and measured data. Calibration of the model is therefore absolutely necessary. Input parameters can be varied and uncertainty ranges due to the vagueness of the information source or measurement are inevitable. This indicates that the basin modeler cannot provide the one and only “true” model. The process of calibrating the model can be done in many ways, however, and a variety of different combinations of parameter settings can often lead to the same result. Lerche (1988) introduced an inverse method aiming at finding the simplest model that best fits all observed calibration data. The modelling community, however, seems not to have adopted this philosophy and by and large trial and error still appears to be the predominant method for calibration.

In this article the calibration of basin models for maturity data of sediments caused by thermal stress is addressed. The amount of thermal stress a sedimentary unit has been subjected to through time is to some extent recorded in vitrinite particles, if present. With increasing thermal stress the vitrinite alters character systematically in terms of its ability to reflect light. Vitrinite reflectance (VR_r, R_r, R_o) can directly be measured and is expressed as a percentage value (Taylor et al. 1998). Sweeney and Burnham (1990) developed the EASY%Ro pseudo-kinetic algorithm for calculating thermal maturity with increasing thermal influence somewhat similar to the observed maturation of vitrinite. The EASY%Ro algorithm is now widely used in basin models which are calibrated by comparing calculated EASY%Ro and real vitrinite reflectance data.

Three parameters are most critical for adjusting the calculated maturity trend: temperature distribution in the basin mainly controlled by the basal heat flow through time, the burial depth of sediments and time as the integrating factor of the equation (Yalcin et al., 1997). The heat flow directly indicates the amount of heat affecting the sedimentary package and controls the geothermal gradient at any time. In those basins or basinal areas with no or only minor erosional events burial depth and time are well resolved by the stratigraphy. In such a case the heat flow history is often the most critical and uncertain parameter to investigate.

In most cases measured vitrinite reflectance increases with depth, but with some scatter, i.e. there is no well defined trend. Scattering of data is less pronounced for coals than for dispersed vitrinite particles (Scheidt and Littke, 1989) and is due to the presence of different vitrinite precursor material, allochthonous vitrinites or local heating events along faults.

A calibration workflow has been devised that starts with a simple assumption of a constant heat flow history and systematically builds complexity to reveal complex behaviors. Of course the complexity and range of the likely possibilities is controlled by the scatter of the measured data points. Calibration points with a large scatter or few calibration points allow a wider range of possible heat flow histories whereas many data points which follow a well defined trend may more likely lead to a solution with small uncertainty ranges. Nevertheless any investigated heat flow history is not the truth but just one realization of many equally likely scenarios.

Using only trial and error with the basin modelling software is very time consuming and finding the “best fit” heat flow history is not guaranteed. Usually the process is stopped at what appears to be a “reasonable fit”.

To avoid large numbers of model runs with the basin modelling software a simplified algorithm introduced by Thomsen and Noeth (2001) is used here to calculate the maturation of vitrinite.

The scatter in the observed data is concretized by calculating the Mean Squared Residual (MSR) after Lerche (1991) where observed maturity data is plotted against a maturation trend line calculated using a simple equation. After the determination of the “best fit” of the varied input parameter the simple model is mapped back into heat flow values which can be used for the complex maturity calculation in the basin modelling software.

The first step of the calibration process provides a “best fit” of a constant heat flow history. This is the simplest solution but not necessarily detailed enough for capturing the true complexity of the thermal history being sought. After using the determined constant basal heat flow when running the model a temperature-depth trend at the present day is obtained and compared to the present day measured bore hole temperatures. If there is a good match between the calculated and measured temperatures using the “best fit” constant heat flow derived from the vitrinite reflectance data and at the same time good agreement between the computed and observed maturity trend there is nothing in the vitrinite reflectance data warranting a more complex heat flow history. This does not, however, rule out a much more complex history. If the calculated maturity trend does not fit the measured vitrinite reflectance data or the calculated present day temperature-depth trend does not fit the measured temperatures a more detailed investigation needs to be carried out.

In principal all uncertain parameters can be investigated in the same manner one at a time. Subsequent MSR calculations for the fit of modeled to observed data give information about the quality and improvement possible after each refining step. The end of the refining process is given by the step after which no improvement of the MSR is achievable.

3.3 Methods

3.3.1 Vitrinite reflectance

In a numerical basin model the thermal maturation of sediments is calibrated by comparing calculated maturity with measured vitrinite reflectance data and obtaining a “best fit”. Vitrinite is a coalification product of humic substances, which originate from the lignin and cellulose of plant cell walls (Taylor et al., 1998). Vitrinite particles react on thermal stress with systematically increasing optical reflectance. This reaction is assumed to be irreversible and therefore only the highest thermal imprint can be seen. Vitrinite reflectance measurements for the two case studies were previously published by Beha et al. (2007) and performed following standard procedures (Taylor et al., 1998).

3.3.2 Basin modelling

Over the past nearly 30 years basin modelling has become a widely used practical tool in geology, especially in petroleum exploration where predicting the dynamic evolution of thermal maturity of sediments and the corresponding transformation of organic material into hydrocarbons is essential.

For simulation of realistic scenarios, the present day state, as interpreted from 2D and 3D seismic needs to be converted into numerical values. Combined with well stratigraphies it forms the basis for building 1D, 2D or 3D basin models. Thus geological, geophysical, geochemical and thermodynamic data are used to constrain such models used to quantify the processes at work during the formation of sedimentary basins. Forward modelling enables us to obtain results from different times during basin evolution and thermal maturation of the sediments. Significant work developing and outlining the framework for the present state of basin modelling was published by Yükler et al. (1978), Nakayama and Van Siclen (1981), Welte and Yükler (1981), Bethke (1985), Nakayama and Lerche (1987), Welte and Yalcin (1987), Lerche (1990a,b), Thomsen (1994) and Welte et al. (1997).

In this study the PetroMod suite of modelling software from IES GmbH, Germany, is used for calculating the maturity trends. For computation of vitrinite reflectance from temperature histories, the software uses the EASY%Ro algorithm of Sweeney and Burnham (1990) which is based on a first order Arrhenius equation which takes the three basin model input parameters temperature, burial depth and time into account. In PetroMod vitrinite reflectance values between 0.3 and 4.5% VR_r can be calculated.

3.3.3 Pseudo-inverse method

For finding the simplest heat flow history that best describes observations the pseudo-inverse method introduced by Thomsen and Noeth (2001) was used. Figure 3.1 shows the basic concept for the method.

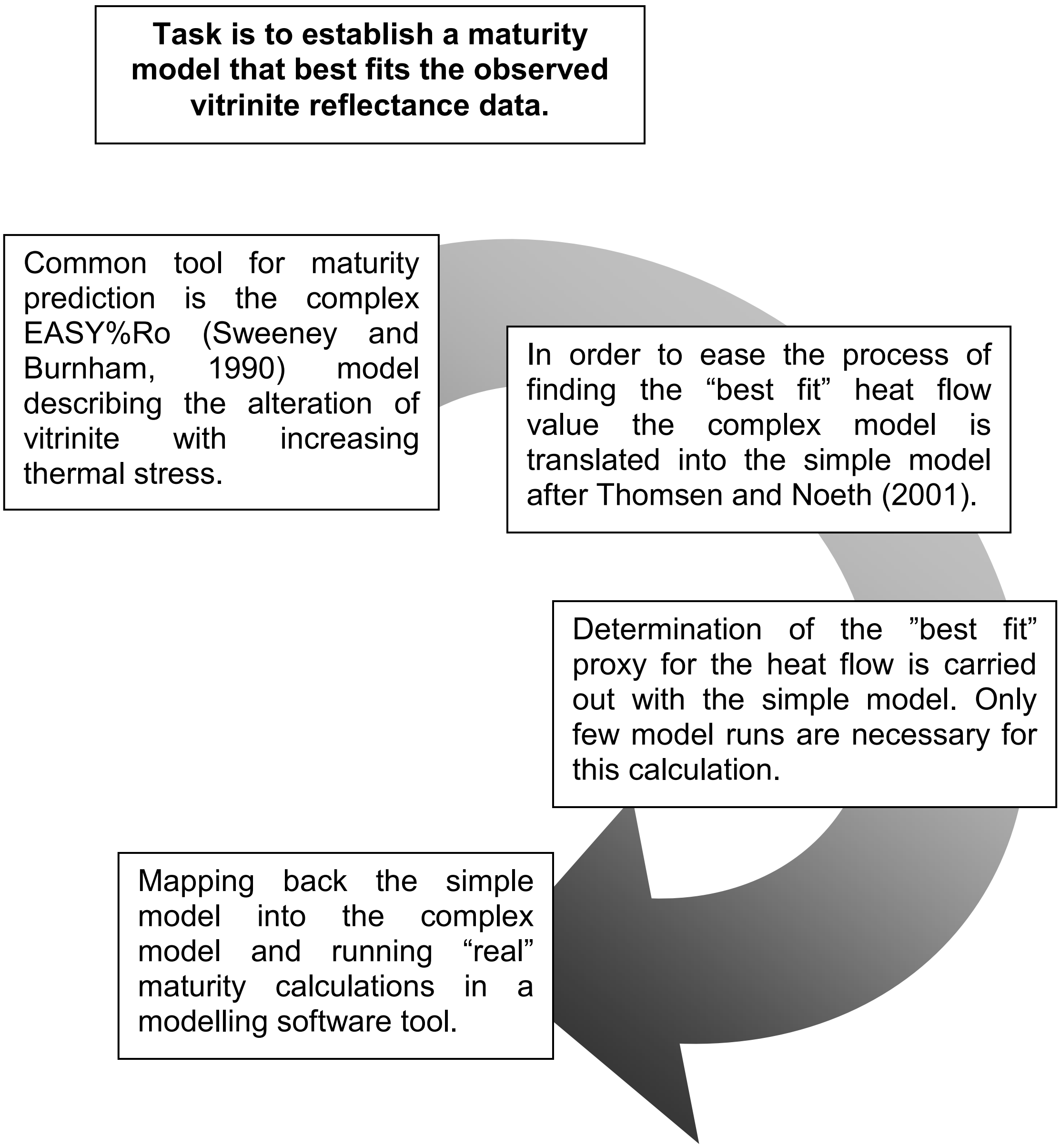

Figure 3.1: Concept of the calculation of the "best fit" heat flow model to best fit the observed vitrinite reflectance data.

On figure 3.2 the reader is introduced graphically to the workflow. A very detailed description of the method was published by Thomsen and Noeth (2001).

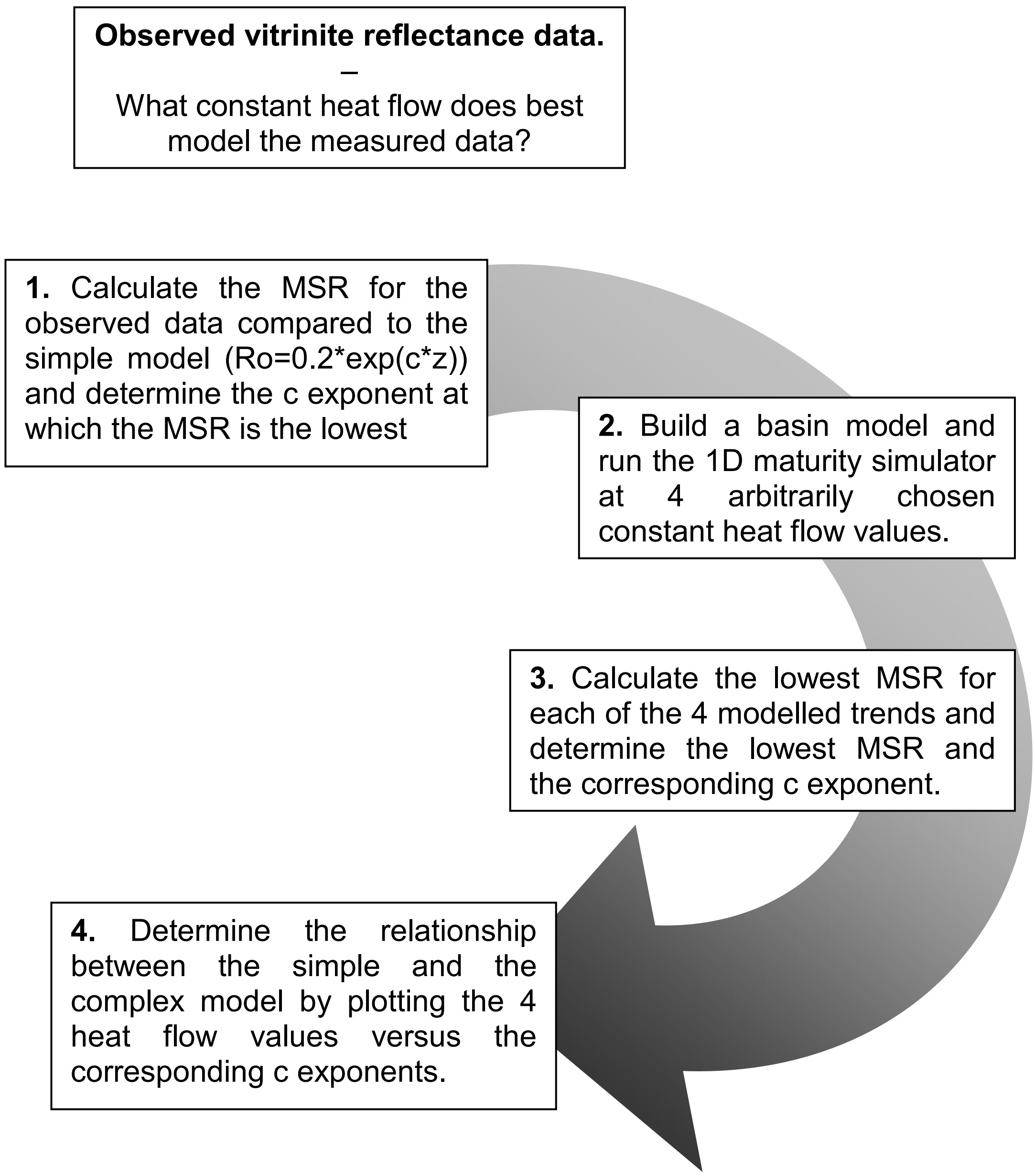

Figure 3.2: Workflow of the four step procedure for finding the ”best fit” heat flow history.

First step of the four step workflow is mapping the real or complex system like the EASY%Ro algorithm (Sweeney and Burnham, 1990) into a simple synthetic model for vitrinite reflectance vs. depth trends. The simple model is expressed by equation 3.1 in which z is the depth and c is the exponent varied during the investigation procedure.

$$R_o = 0.2 \cdot e^{(c \cdot z)} \tag{3.1}$$

The MSR (equation 3.2) for the misfit of the observed data compared with the modelled data is calculated for a number of different maturity trends created by applying various c exponents to equation 3.1.

$$MSR = \frac{1}{N}\sum_{i=1}^{N}(R_{obs} - R_{cal})^2 \tag{3.2}$$

Results for these calculations are plotted in a MSR vs. c exponent diagram (see figure 3.4) and a cubic spline is used for interpolation between the investigated points in order to obtain a continuous representation of the MSR of the simple model fit to the observations, in this case vitrinite reflectance. The c exponent with which the lowest MSR for the misfit of the observed data compared with the simple model was calculated is the c exponent used for the simple model that “best” fits the measured data.

Four 1D basin models with arbitrarily varied constant heat flow values are run in *step two*. About ten depth - R_o data pairs are collected from the resulting maturity trends in order to calculate the MSR for the misfit of the maturity trends calculated with the complex model compared with the simple model for each constant heat flow value in *step three* of the workflow. Each of the four MSR curves representing the different heat flows used in the basin modelling software shows a well defined minimum MSR value, indicating a “best fit” at the c exponent with which the simple model is resolved best in the observed data, in this case EASY%Ro maturity trends. *Step four* is plotting the four constant heat flow values versus the respective c exponents. This step allows mapping the simple system back into the complex system. For that reason a function is established linking the four heat flow – c exponent pairs. The “best fit” constant heat flow value for the modelling software tool is found by the above defined relationship between heat flow values (real or complex model) and c exponents (simple or synthetic model) on the “best fit” c exponent found in step one. Later on we discuss simple and complex *heat flow histories* which should not be confused with the simple or complex *models for vitrinite maturity prediction*.

Noeth et al. (2002) and Huvaz et al. (2007) included the pseudo inverse method in their investigations on “best fit” thermal histories and applied it on different geological settings.

3.3.4 Calibration procedure

As addressed in the introduction, a workflow is followed where starting with the simple model the observed maturity data is matched by gradually increasing the complexity of the model until the limits of resolution of the heat flow history in the basin model in the observed data are determined. First step is the calculation of the MSR for the modeled trend line from the simple model compared with the measured data (Thomsen and Noeth, 2001). The magnitude of the minimum MSR is a first indicator of the achievable resolution of heat flow history in the measured data compared to a “perfect” simple maturity model. The higher the minimum MSR value the greater the misfit and the wider the acceptable range of changes of resolved parameters, for instance the heat flow.

The MSR is calculated for four discrete heat flow values and to obtain a continuous representation of the MSR for the observed data a cubic spline is applied to interpolate between the investigated points.

The shape of the MSR curve is an indication of how sensitive the model is to variations in the parameter being investigated. A wide range of low MSR values indicates a very insensitive behavior of the system to variations in the investigated parameter, whereas steep flanks on the MSR curve with a well defined narrow minimum indicate high sensitivity to changes in the parameter. A difference in the steepness of slope on either side of the minimum indicates in which direction parameter change has the bigger impact on the model results. A detailed description of the MSR calculation work flow can be found in Thomsen and Noeth (2001).

3.4 Case studies

To illustrate the procedure two wells have been selected as examples. The wells are located in the Horn Graben in the Danish North Sea. Each well was modeled using IES 1D PetroMod. Detailed information on location, model building process, input parameters and available calibration data are described in Beha et al. (2007). Figure 3.3 shows the available temperature and vitrinite reflectance calibration data for the two example wells.

Both wells show much higher calculated palaeo temperatures than present day temperatures when the "best fit" constant heat flow is calibrated for the maturity data. This means that the Horn Graben area must have been affected by a heat event in the past.

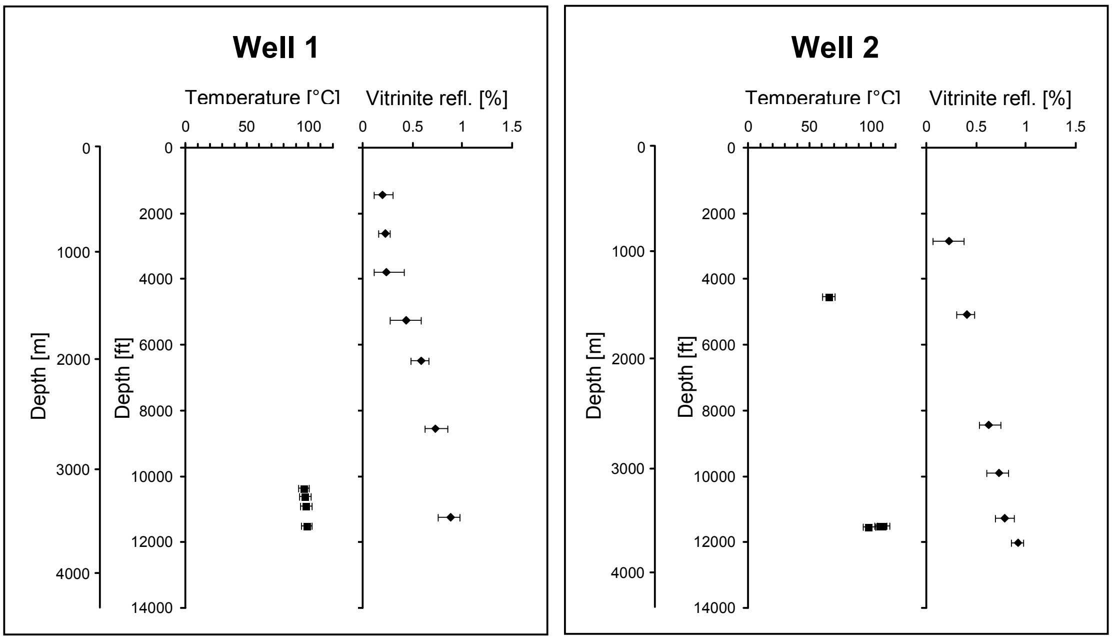

Figure 3.3: Available calibration data for well 1 and well 2.

In this paper we show a quick method to determine a “best fit” heat flow history that can be used for the numerical basin model. We are aiming at finding the simplest model that is in best possible agreement with the measured data.

For both example wells the MSR was calculated for the simple model trend lines compared to the measured data for determining the c exponent with which the simple model fits the observed data best. Well 1 shows a best fit with a c exponent of 0.0001377 at a MSR of 0.00504 (Figure 3.4), whereas the simple model fitted the data of well 2 best with a c exponent of 0.0001269 at a MSR of 0.001594.

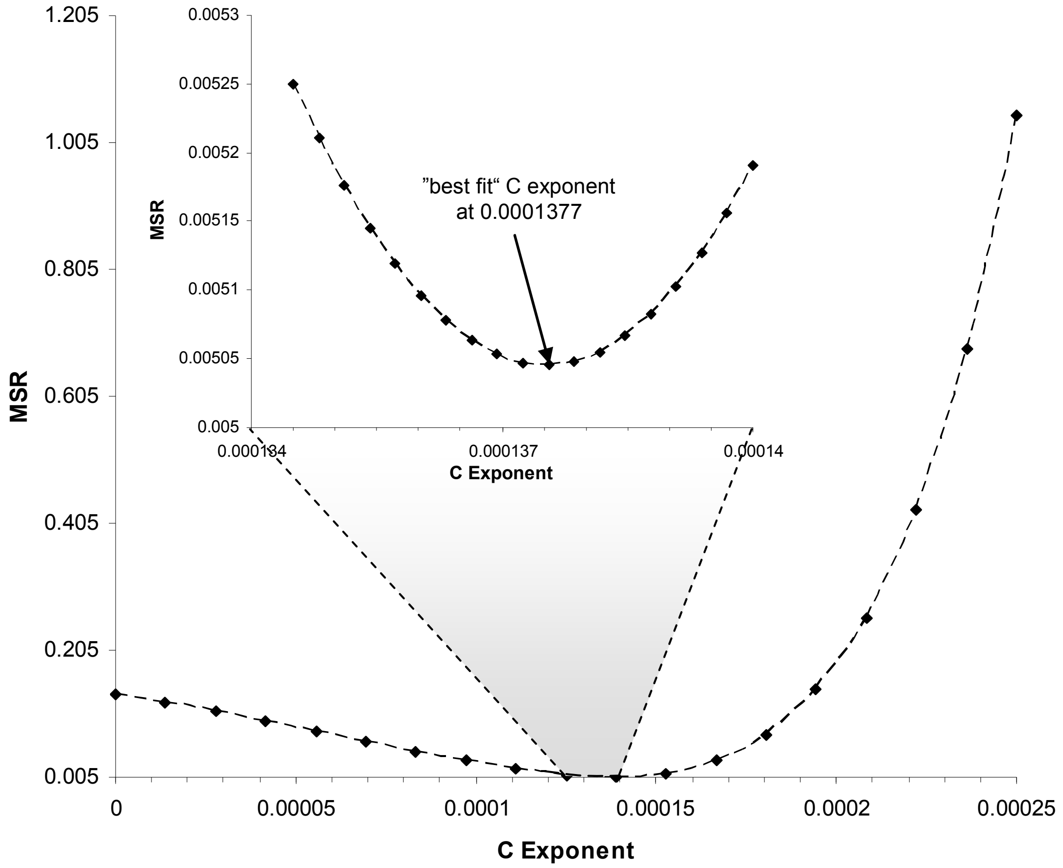

Figure 3.4: MSR calculation results for the simple model compared with the observed vitrinite reflectance data from well 1. A distinct minimum with a c exponent of 0.0001377 is determined. The misfit is quantified in the magnitude of the MSR (0.00504). A similar calculation was conducted for well 2. There a c exponent of 0.0001269 gives a "best fit" with a minimum MSR of 0.001594.

3.4.1 Well 1

The first step, following Thomsen and Noeth (2001) was to calculate the MSR for the calculated trend lines from the simple model compared with the observed data. Subsequently four arbitrarily chosen constant heat flows were used to back-map the simple model into the complex system and finding the "best fit" constant heat flow. Figure 3.5 shows the four MSR curves calculated for the simple model compared to the measured data. This procedure gave a "best fit" constant heat flow of 59.2 mW/m^2 at the c exponent for well 1 to model the observed maturity data best (Figure 3.6).

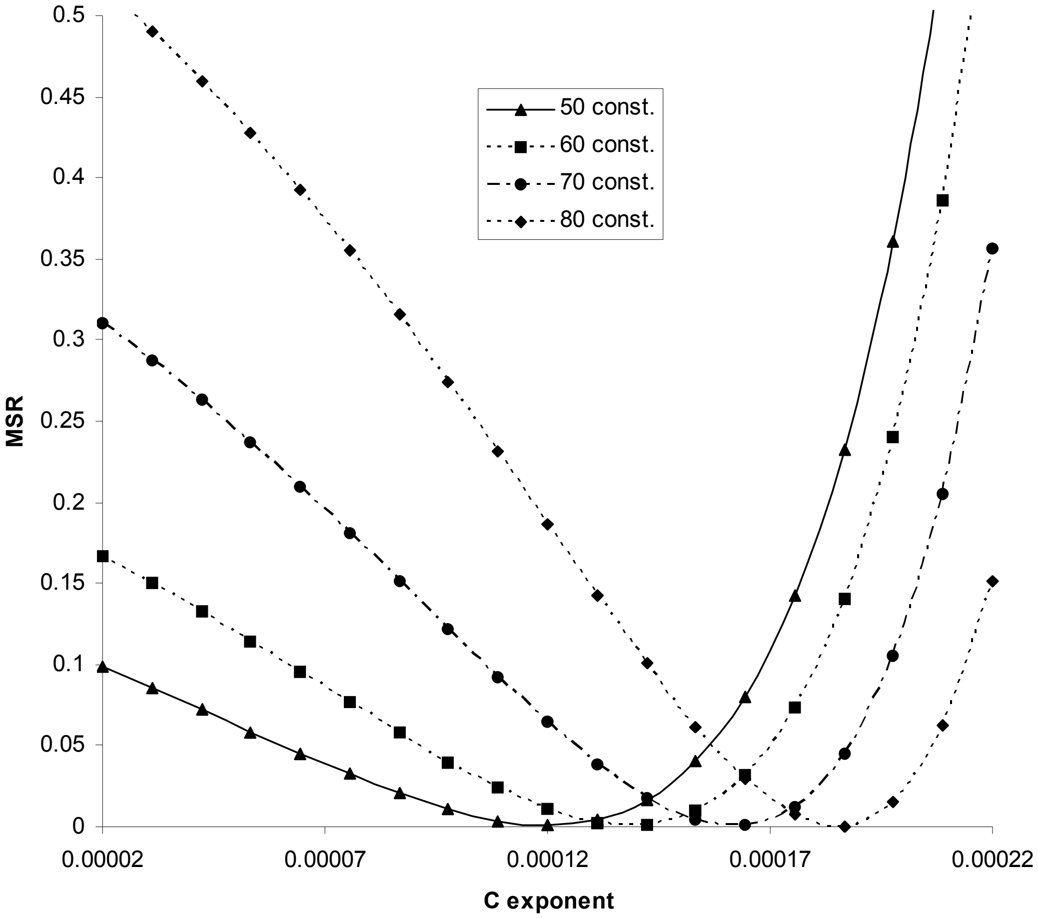

Figure 3.5: MSR calculation for four arbitrary chosen constant heat flow values. The MSR was calculated for the simple model compared to the observed maturity data in well 1.

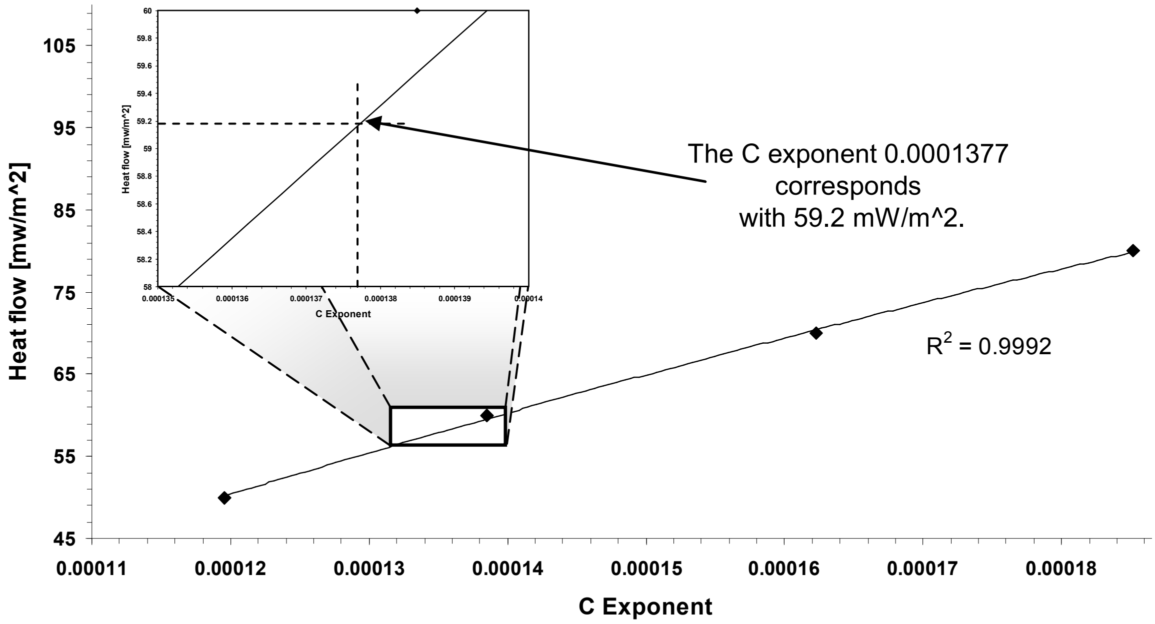

Figure 3.6: Heat flow vs. c exponent plot for back mapping of the simple model to the complex. Here, the "best fit" c exponent for well 1 gives a "best fit" constant heat flow of 59.2 mW/m^2.

After running the 1D basin model with the "best fit" constant heat flow the present day modeled temperature profile does not match the observed bore hole temperature data. The calculated temperatures are consistently above the measured temperatures. To find the heat flow that provides a best fit to the measured temperatures the MSR was calculated for the modeled geothermal gradient compared to the measured data (Figure 3.7). Again, a number of models with different constant heat flow values were run. A heat flow of 50.5 mW/m^2 was found to give the best agreement between modeled present day temperatures and measured temperature data. Hence, this value was set as the "best fit" present day heat flow.

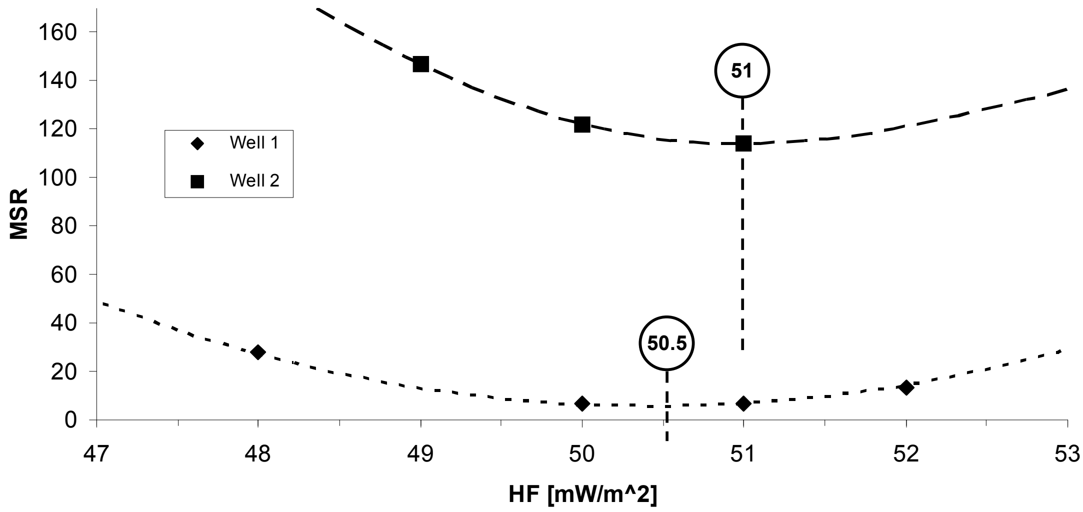

Figure 3.7: MSR calculation results for present day temperature calibration procedure. The MSR was calculated for different modeled temperatures compared with measured temperature data. Results for both wells are shown in this plot. The different level of misfit of the modeled data compared with the measured temperatures is captured in the different MSR values.

The lower constant heat flow expectedly has a big impact on the calculated maturity data which now is much too low compared with the measured Ro data.

The discrepancy between the heat flow necessary to model the observed maturity trend and heat flow necessary for obtaining the temperature observed present day leads to the hypothesis that the sedimentary rocks must have experienced higher heat flow in this area in the past. According to the geologic history described in Beha et al. (2007) it is very likely that during the time of initial basin formation in early Triassic times heat flow was higher which has increased the maturity of the sediments. A higher heat flow in the past can be encountered by applying a crustal stretching model such as that of McKenzie (1978) for calculating a possible heat flow history. Various basin characteristic input parameters need to be estimated and used for determining a possible model for a detailed heat flow history. A major question, however, is how good the resolution of such a complex model is in the observed data - especially in the case where no precise information exists on the basin specific parameters. The approach in this article is to resolve the heat flow history in the observed data by continuously improving the MSR through further partitioning of heat flow values through time.

Following the procedure outlined in previous chapters a second step is introduced to find the heat flow at 248.2 Ma, the earliest point captured in the basin model, that best fits the observed Ro trend. In the modelling a linear decay of the heat flow from model start to present is assumed. Now, not the entire constant heat flow history is varied but only the heat flow at the model start is changed in the four calculations that are necessary for mapping the simple model back to the complex model. In the model the heat flow at 248.2 Ma before present day was randomly set to 70, 80, 90 and 110 mW/m^2 in order to capture a wide range in maximum heat flow as indicated by a variation in stretching factors, β, according to the McKenzie (1978) model.

After running the four cases with the 1D basin model a MSR curve was calculated for fitting the simple model to the 1D model for each case and the c exponent at the lowest MSR for each model run plotted against the value of the varied parameter. A trend line was then determined for the back mapping process from the simple to the complex model. A MSR curve for the observed data is constructed and used to determine the heat flow at the start of the model that best fits the observations. In well 1 a “best fit” was obtained at a starting heat flow of 89.4 mW/m^2.

After this second step in the investigation the heat flow history is now defined by a high start value of 89.4 mW/m^2 248.2 Ma ago and a relatively low present day value of 50.5 mW/m^2 with a linear decline through time. This heat flow model is very simplistic and differs from a traditional rifting heat flow history. To achieve a rift model the behavior of the decline through time needs to be investigated. Again, the key question is if a rift type heat flow model can be resolved in the observed VR_r data based on a calculated maturity trend using EASY%Ro.

To address this problem the same procedure is used to determine the time at which the difference between the heat flow value at the model start and the value at present day is halved. Thus a heat flow value of 69.95 mW/m^2 is set to be reached at four arbitrarily chosen time steps between 1 and 248.2 Ma. In this example 10, 80, 180 and 240 Ma before present day were chosen and the lowest MSR for each of the four models was calculated. After mapping the simple model back to the complex the time for a heat flow value of 69.95 mW/m^2 providing a best fit to the Ro data was determined to be 122.9 Ma.

This point is located on the straight decline heat flow history determined one refining step before and therefore supports the simplistic heat flow history applied to the basin model.

To investigate the impact on the quality of the heat flow model the refining steps had on the calculated Ro compared with the measured vitrinite data a MSR calculation for the real model and the observed data was calculated for every refining step. A distinct MSR value indicates the level of misfit of the model compared to the control data, here VR_r. MSR values for the "best fit" constant heat flow history and the two refining steps were calculated and the results are shown in figure 3.8. A relatively low MSR was achieved already for the "best fit" constant heat flow model which was only calibrated with the observed maturity data.

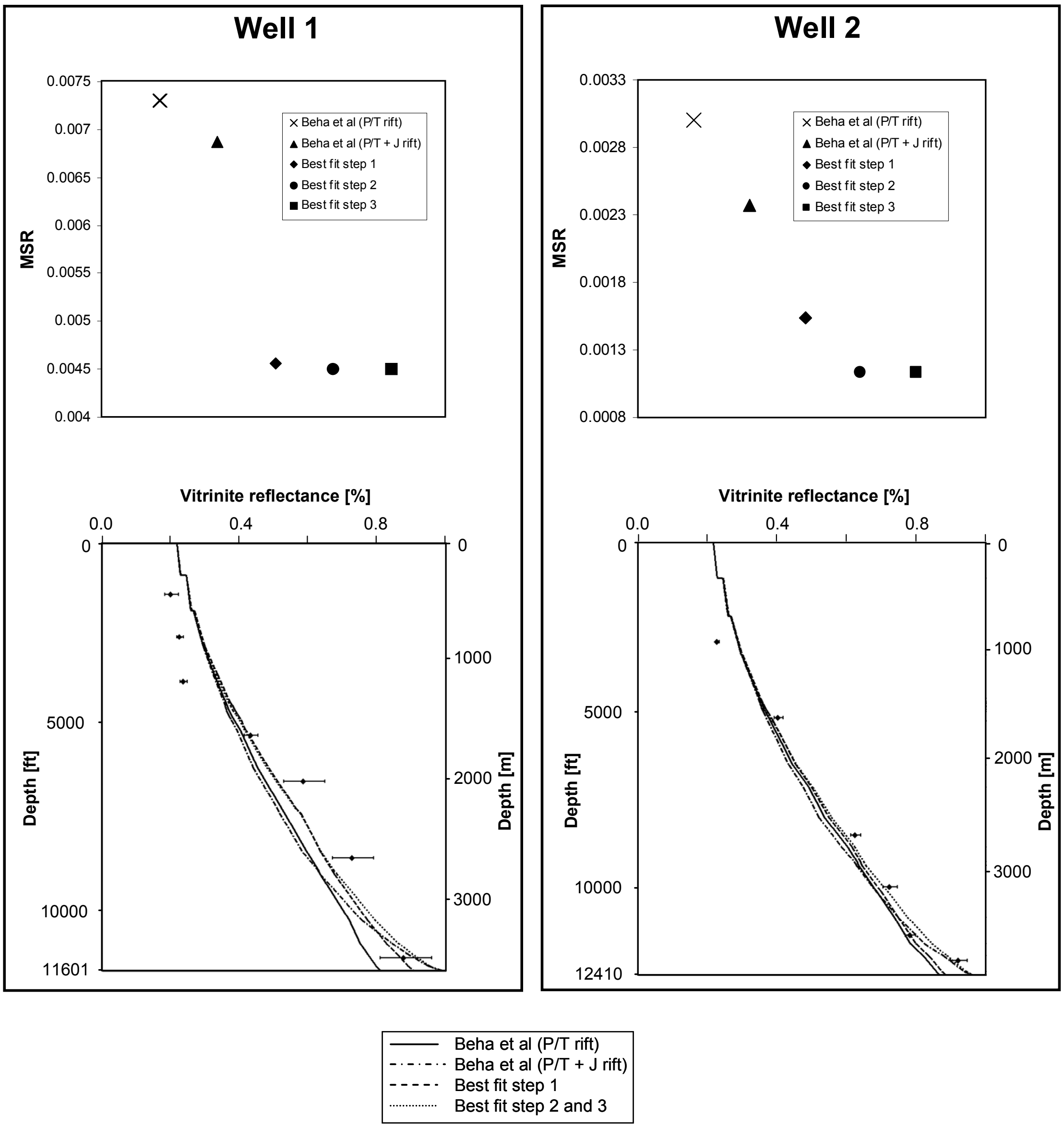

Figure 3.8: Evolution of the misfit of the modeled maturity data compared with the measured vitrinite reflectance data. Modelling results are shown for both wells.

The MSR for the second step with a high heat flow in the past linearly declining to a low heat flow value at present day showed a lower MSR. The third step set the time at which the difference between the two heat flow values at the beginning of the model and at present day was halved. No improvement of the MSR was obtained by adding this refinement. Within the framework of this exercise the limit of resolution of heat flow in the observed data was reached. In figure 3.9 the “best fit” simplistic heat flow history is shown and compared with the rift type complex heat flow histories including either one or even two separate rifting events published by Beha et al (2007).

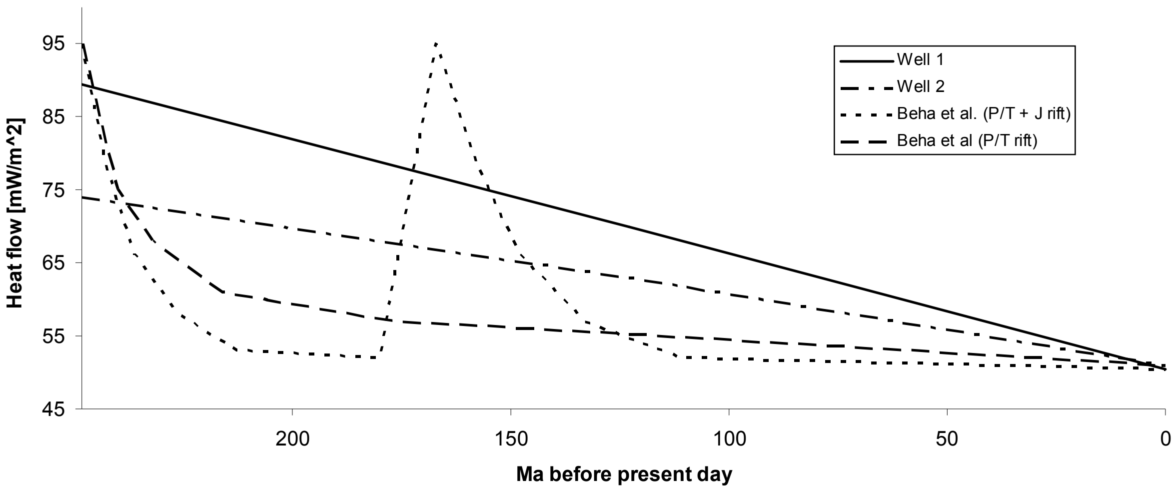

Figure 3.9: Distribution of heat flow values through time for the different refinement steps and earlier published heat flow histories. This figure shows the “best fit” heat flow history for both wells.

3.4.2 Well 2

The same procedure was applied to well 2, an adjacent well in the Horn Graben. Again, the model building process, input parameters and available calibration data are described in Beha et al. (2007).

A “best fit” constant heat flow value of 55.59 mW/m^2 was determined in the first step where the model was only calibrated against observed vitrinite data. This result corresponds well with the “best fit” constant heat flow value for well 1 (59.2 mW/m^2). Also in this well the calculated temperature trend for the present day shows higher temperatures than measured and needed to be adjusted in order to match the present day heat flow derived from the temperature data. Again this hints to the fact that the simple constant heat flow model is not an adequate model in this part of the Horn Graben and higher heat flow conditions must have occurred sometime in the past.

The “best fit” present day heat flow was found by calculating the MSR for temperature data under varying constant heat flow values. A constant heat flow of 51 mW/m^2 (see figure 3.7) gives a good agreement with the measured bore hole temperature data and matches the present day heat flow value of the well 1 model (50.5 mW/m^2). Consequently 51 mW/m^2 was used for the present day heat flow. In line with the findings in well 1 and the geologic history of the basin a maximum heat flow value at the start of the model and the type of decline to present day value needs to be determined. Following the procedure described earlier a value of 74 mW/m^2 was determined in well 2 to be the “best fit” maximum heat flow at the start of the model. Obviously there is a big difference between the maximum heat flow event of well 1 (89.4 mW/m^2) and well 2 (74 mW/m^2). Due to the geographical vicinity of the two wells the reason for this is rather found in the scatter of the observed maturity used as calibration data than in a totally different geological setting.

Mathematically of course it is interesting to see, how many further heat flow values can be calculated to best map the measured data. Again, the improvement of the calculated maturity trends is monitored by calculating the MSR for the modeled maturity and the measured VR_r data.

Consequently a third MSR was calculated to determine the time at which the difference between the maximum heat flow at model start and the low present day heat flow is halved. Result of this third refining step is a heat flow of 63 mW/m^2 at a time of 122.5 Ma. By plotting the calculated intermediate step into the heat flow history of wells 2 it is again obvious that there is no deviation from a linear decay beginning at the maximum heat flow value at the start of the model to the lower value at present day. Also the MSR calculation for the complex model and the observed data did not show any improvement in the misfit after adding the information from the last refining step in the simplistic heat flow history (see figure 3.8). Again the limit of resolution of heat flow in the observed data was reached. Figure 3.9 shows the simplistic heat flow history that matches the observed data best compared to the simplistic heat flow history determined for well1 and the complex heat flow histories published by Beha et al (2007).

3.5 Discussion

The study shows that only the present day heat flow can be determined by comparing measured temperature and Ro data with the modelling results. Complexity can not be added to the heat flow history applying basin modelling results. Additional information for timing and magnitude of possible heat anomalies in the past must come from different sources and subsequently integrated into the existing heat flow model.

A key question for hydrocarbon exploration aspects is how temperature and maturity evolve through time in possible source rock units since these factors actively steer the amount and timing of hydrocarbon transformation from kerogen. Figure 3.10 shows a comparison of calculated temperature and maturity through basin history for well 1 for different heat flow histories.

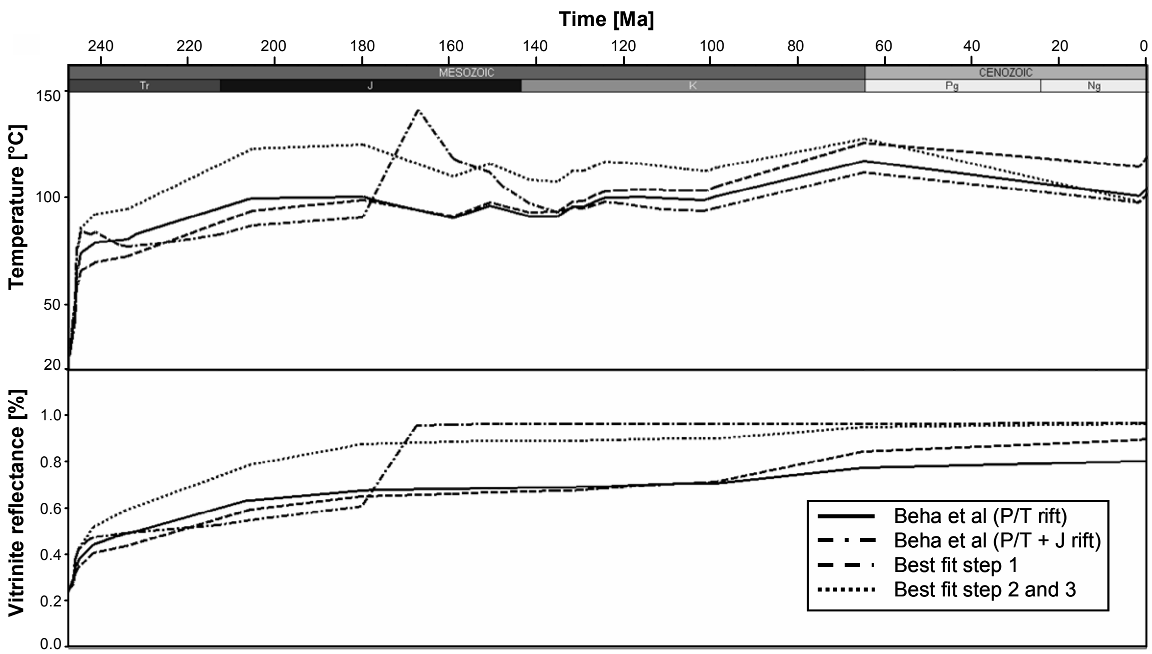

Figure 3.10: Temperature and maturation evolution through time. The deeply buried shale of Induan age in well 1 is monitored. A similar situation is seen in well 2.

As the deepest layer, a shale of early Induan age was monitored. A trend line is shown for the refining steps in heat flow history described in the "Case studies" section of this article and the simple and complex heat flow histories earlier applied to the wells in the Horn Graben by Beha et al. (2007). A clear distinction between the different heat flow conditions is visible on the chart. The temperature curve for the complex heat flow history with the initial rift heat flow anomaly included shows a temperature evolution that is mainly controlled by subsidence and burial of the sediments. The heat flow history which includes a second heat event in the Early to Middle Jurassic shows a dramatic increase in temperature during this time. A constant "best fit" heat flow history reacts similar to the initial heat flow history with only one heat anomaly at model start. The temperature for the "best fit" heat flow histories for refinement steps 2 and 3 evolves simultaneously due to the same heat flow distribution through time. The chart shows a similar pattern for vitrinite reflectance evolution. The earlier published heat flow history with one heat flow anomaly and the "best fit" constant heat flow history have the lowest impact on alteration of vitrinite particles. A very different situation is seen with the complex earlier heat flow history with two heat flow peaks. An increase of more than 0.25% in reflectance appeared within a very short time during the Jurassic. Following this result the present day maturity of the lower Induan sediments was already reached some 170 million years ago. Maturation of the observed stratigraphic unit shows a similar but somewhat smoother trend for the "best fit" heat flow histories for the 2nd and 3rd refinement step. Also in this case the sediments reached a high grade of maturity at a very early stage. A similar situation is seen in well 2.

The present day situation is not very different in the investigated cases, but as addressed at the beginning of this section the different maturation history would certainly have an impact on hydrocarbon generation in source rocks.

3.6 Conclusions

The MSR method is a tool that allows monitoring the misfit of calculated trend lines compared with measured data, in this case vitrinite reflectance. It supports investigating the resolution of heat flow history in observed data in basin models. In both case studies it was clearly shown that from a mathematical point of view an improvement of the calculated trends was obtained by applying simplistic models. Once a "best fit" model with a high heat flow value at the model start and a lower value at present day was found, no improvement of the modeled data compared to the observed was found. Figure 3.8 in the "Case studies" section of this article shows an improvement of the results compared to the heat flow histories that have been applied in an earlier study by Beha et al (2007). The improvement of the misfit can be seen in both wells.

The study clearly shows the limitations of resolving the calculated trend lines in the observed data by applying the EASY%Ro algorithm from Sweeney and Burnham (1990). Heat anomalies caused by varying heat flow in the past can not be determined using standard basin modelling tools. Especially information on the timing of heat events need to be implied from other studies. However, the maximum magnitude of these events subsequently can be determined by following a comparable workflow to the one described in the "calibration procedure" section of this paper.

In general the MSR calculation method can be used for any kind of investigation when boundary conditions are changed for instance the "best fit" burial history, especially when extensional erosion events occurred during basin evolution.

4 Verification of a simple model for the prediction of vitrinite maturity ranges in basin modelling studies.

4.1 Abstract

Basin models are widely used to investigate the thermal maturity of sediments within a basin. Thermal maturation is directly controlled by the temperature field in the basin defined by basal heat flow, burial depth and time. For models to be predictive with respect to maturity they need calibration against thermal indicators measured at present day. Vitrinite reflectance is a broadly accepted thermal indicator believed to provide information on the total amount of heat energy felt by the vitrinite particles in the course of basin evolution. Hence the amount and distribution of the cumulative heat energy mainly controlled by basal heat flow is object of the investigation. Constant heat flow through time is the simplest conceptual representation of heat flow history. However, even calibrating numerical basin models with a constant heat flow history is often a very time consuming process as heat flow values need to be changed for every model calculation and results need to be compared to observations until an acceptable match is achieved. To shorten this procedure a simple model

introduced by Thomsen and Noeth (2001) is used to investigate a very quick estimation of a “best fit” constant heat flow value. In contrast to the complex kinetic model for thermal maturity prediction in basin modelling software this simple model is based on a simple equation. Without extensive calculation time the simple model allows drawing preliminary conclusions for constant heat flow histories that will match the observed data best. Further development of this methodology led to the “Instant Sensitivity Analysis Tool” introduced in this article which allows in addition to the “best fit” determination of acceptable maximum and minimum ranges for constant heat flow to be determined very quickly. The impacts on hydrocarbon generation and expulsion in the consequent heat flow study are obtained by applying the results of the simple model investigations to the complex basin model and simulating hydrocarbon generation using standard kinetics. To validate the described sensitivity analysis in the simple system, the behaviour of both the simple and the complex model for maturity prediction was investigated and it is shown that the complex calculation in the basin modelling software responds in the same way to changes in the heat flow as the simple maturation model to the heat flow proxy.

Case studies have been conducted on two wells in the Danish Horn Graben to investigate the behaviour of both the simple and the complex model with the aim to verify the assumption that quick and simple identified constant heat flow values give good evidence for applying the “best fit”, minimum and maximum heat flow values to the complex calculation in the basin modelling software tool.

4.2 Introduction

Basin modelling is commonly used in quantitative petroleum studies. Numerous authors used basin modelling for investigation of various processes at work during basin evolution (Doré et al., 1993, Hertle and Littke, 2000, Littke et al., 2000, Ungerer et al., 1990, Schwarzer and Littke, 2007, Tissot et al., 1987 and Waples, 1998). At the beginning of every modelling project calibration of the model to measured data valid in the specific region of interest is important and provides the level of confidence that is associated with modelling results. Lithology linked to the stratigraphic unit, calibration data and thermal history are basic information for the numerical model and the resulting model is only as good as the calculated results match the observed and measured data and the validity of the underlying geologic model. Vitrinite reflectance data are usually available and often used as a standard thermal indicator thus the focus in this article is the calibration of basin models to measured vitrinite reflectance data. In most basin modelling studies the calibration results in a visual “best fit” calculated trend line without discussion of resolution of information or sensitivity to changes in the heat flow model.

In principle the input parameters for basin models can be varied and uncertainty ranges due to vagueness of the information source or measurement are inevitable (Nielsen, 1996). This implies that the basin modelling results may not necessarily be correct by achieving a good visual agreement with observed control data. In fact a lot of different parameter settings may produce very similar results. For finding the simplest model that best agrees with the measured data Lerche (1988) developed an inverse method in order to avoid over-stated confidence in modelling results which try to resolve calculated maturity trends in observed data by applying complicated parameter variations through time. The pseudo-inverse method used for this article is based on a very simple equation for maturity prediction in basin models introduced by Thomsen and Noeth (2001). It allows obtaining “best fit” values for parameters investigated in a very short time. Results are based on a mathematical analysis rather than the subjective eye of the basin modeller in charge. In contrast to this simple model for maturity prediction stands the complex model based on a complex kinetic describing the alteration of vitrinite under various boundary conditions. An example for the complex model is the EASY%Ro algorithm (Sweeney and Burnham, 1990) used in the PetroMod basin modelling suite.

For the purpose of testing the optimization and speeding up the calibration procedure two 1D basin models in the Danish North Sea have been used. Model building process and basic input parameters are described in Beha et al. (2007). In this article we aimed at devise a procedure for finding the simplest heat flow history that best agrees with the observed data. A “best fit” using a constant heat flow history for each of the two wells will be calculated following the four steps described by Thomson and Noeth (2001). Calculations of the Mean Squared Residual (MSR) as a clear indicator of the misfit of the calculated compared to the observed data were conducted for both, the simple and the complex model. Cross plotting the results shows a linear correlation which shows that varying the c exponent in the simple model will change the misfit of the predicted trend compared to the measured data points with the same sensitivity than changing the heat flow values in the complex basin modelling tool within the investigated range. This result allows introducing the “Instant Sensitivity Analysis Tool”, a very quick and graphically demonstrative method to easily determine a minimum and maximum acceptable range for the constant heat flow applied to the basin model.

4.3 Methods

4.3.1 Vitrinite reflectance

In a numerical basin model the thermal stress is calibrated by comparing calculated maturity with measured thermal indicators. Most commercial models, however, are limited to vitrinite reflectance data. Vitrinite is a coalification product of humic substances, which originate from the lignin and cellulose of plant cell walls (Taylor et al. 1998). Vitrinite particles react on thermal stress with systematically increasing optical reflectance. This reaction is assumed irreversible and depends to a great extent on the highest thermal imprint (Sweeney and Burnham, 1990). Vitrinite reflectance measurements for the presented case studies were carried out on dispersed vitrinite in sediments. Results were previously published by Beha et al. (2007).

4.3.2 Basin modelling

Over the last three decades basin modelling has become a widely used and accepted practical tool in geology, especially in petroleum exploration where predicting the dynamic evolution of thermal maturity of sediments and the corresponding transformation of organic material into hydrocarbons is essential. Significant work developing and outlining the framework for the present state of basin modelling was published by Yükler et al. (1978), Nakayama and Van Siclen (1981), Welte and Yükler (1981), Bethke (1985), Nakayama and Lerche (1987), Welte and Yalcin (1987), Lerche (1990a,b), Thomsen (1994) and Welte et al. (1997).

In this study the PetroMod suite of modelling software from IES GmbH, Germany, was used for calculating the maturity trends. For computation of vitrinite reflectance from temperature histories, the software uses the EASY%Ro algorithm of Sweeney and Burnham (1990) which is based on a first order Arrhenius equation where time and temperature are derived from the three basin model input parameters temperature, burial depth and time. In PetroMod vitrinite reflectance values between 0.3 and 4.5 VR_r can be calculated.

4.3.3 Pseudo-inversion of forward deterministic models

Inversion of 1D basin models helps finding the “best fit” model that best matches the observed data in the area of investigation. Various inversion procedures have been developed for different input parameters important for hydrocarbon potential assessments. Parameters such as palaeoheat flow, stratigraphic age, and parameters governing the fluid-flow, pressure and compaction modelling were investigated by Lerche (1988, 1991), Thomsen et al. (1990) and Thomsen (1994, 1998).

The main advantage of 1D inversion procedures is the short calculation time of only a couple of minutes and a limited number of model runs in the basin modelling software. Limitations to inverse calculations are given by models of higher dimensionality due to much longer computing time.

For the applied workflow generally only four model runs within the basin modelling software are necessary to map back the simple model into the complex system. Finding the "best fit" heat flow value for each of the wells was performed following the workflow introduced by Thomsen and Noeth (2001). Noeth et al. (2002) and Huvaz et al. (2007) included the pseudo inverse method in their investigations on "best fit" thermal histories and applied it on different geological settings.

4.4 Results

4.4.1 Calibration procedure

Calibration of basin models generally is a very time-consuming process. Especially 2D and 3D basin model calculations need extensive time or computing capacity and often end with a visual acceptable calculated heat flow trend that best fits the data in the respective basin modeller's eye.

In this article the two investigated 1D basin models of wells in the Danish North Sea were calibrated against maturity data. Hence variations in constant heat flow values were applied to the basin model. Aim of the study was obtaining a "best fit" heat flow and additional to that a lower and an upper acceptable limit. The simple model introduced by Thomsen and Noeth (2001) was used to shorten the process of calibration. Besides finding a “best fit” this method also allows a mathematical analysis of the goodness of fit between the measured and calculated maturity data.

First the four step workflow was followed to obtain the “best fit” constant heat flow for each of the two wells. The calculated MSR for the “best fit” constant heat flow gives a clear indication of the best achievable match between measured data and calculated trends in the given case of applying constant heat flow histories to the model (Thomsen and Noeth, 2001).

In an additional step the behaviour of the MSR for both, the simple and the complex model was investigated. Therefore ten model runs for both wells were performed with the basin modelling software. MSR calculations for each run have been conducted for both systems, simple and complex. In order to obtain a continuous representation of the MSR of the fit to the observed data a cubic spline is used for interpolating between investigated points.

4.4.2 Well 1

Calibration data available for Well-1 is shown in Figure 4.1. The simple as well as the complex maturity prediction model have been applied to calculate trend lines trying to predict the maturity level of the sediments in the investigated area. The MSR for each parameter change in both systems has been calculated as an expression of the misfit of the calculated trend lines compared to the measured data.

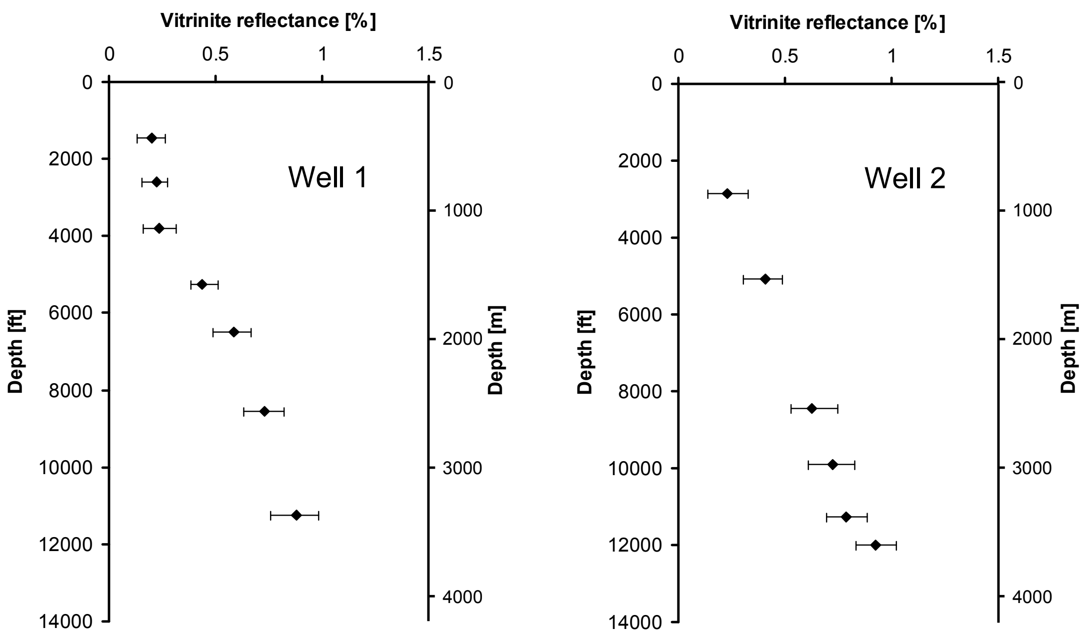

Figure 4.1: Measured vitrinite reflectance data for well 1 and well 2.

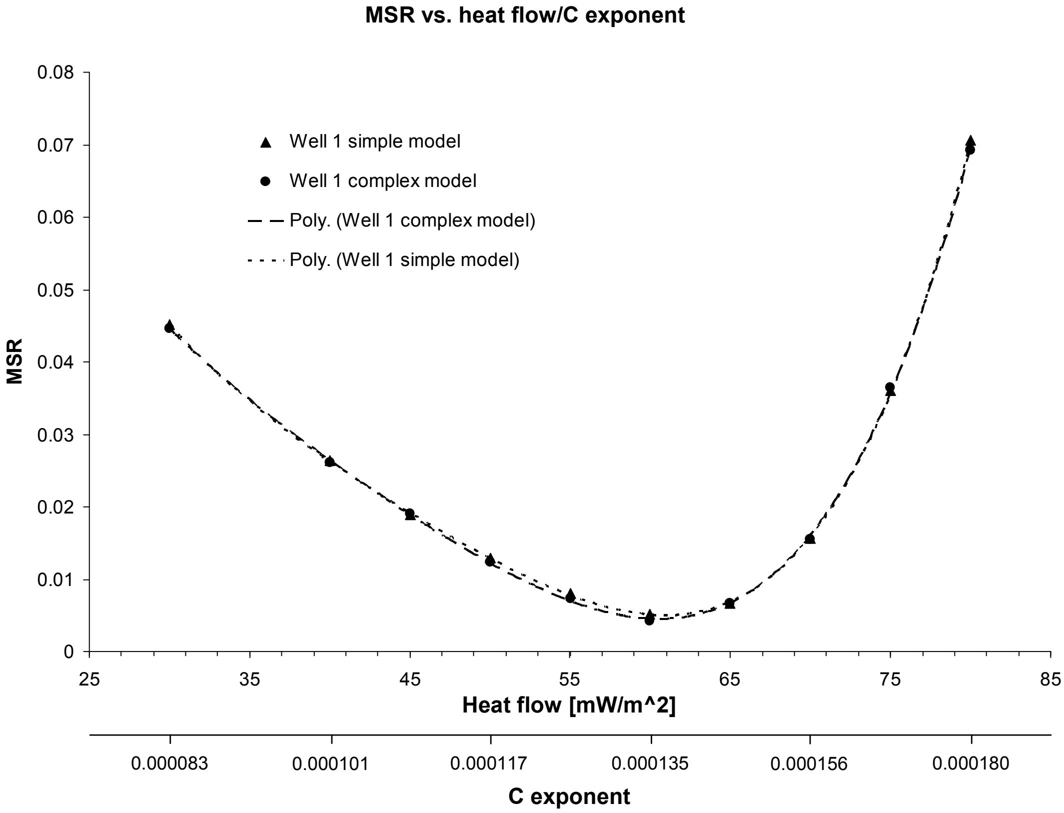

Figure 4.2: MSR calculation results for the varying input parameter heat flow in the complex model or c exponent in the simple model after Thomsen and Noeth (2001). Results are shown for well 1. Please note that the relation between c exponent and heat flow values is non-linear. Comparisons can only be conducted after mapping the simple system into the complex.

Figure 4.2 shows the results of the MSR calculations for the simple and the complex model for well 1. It is obvious that the two systems behave very similar when varying the input parameter. Variation of the c exponent in the simple model and heat flow in the complex model leads to the same grade of mismatch between the observed and the calculated data. The reader has to be aware of the fact that the relation between variation of c exponent and variation of heat flow values is non-linear. The heat flow values are products of the back mapping step from the simple model to the complex model described in Thomsen and Noeth (2001). Figure 4.3 shows the relationship between c exponent and heat flow for well1. A “best fit” heat flow of 61 mW/m^2 was found in case of well 1. Variations in the “best fit” constant heat flows compared to previous calculations in section 3 of this thesis is due to more calculated “c exponent - heat flow” pairs in this second study which give a better definition of the relationship between c exponent and heat flow. The difference is small, though.

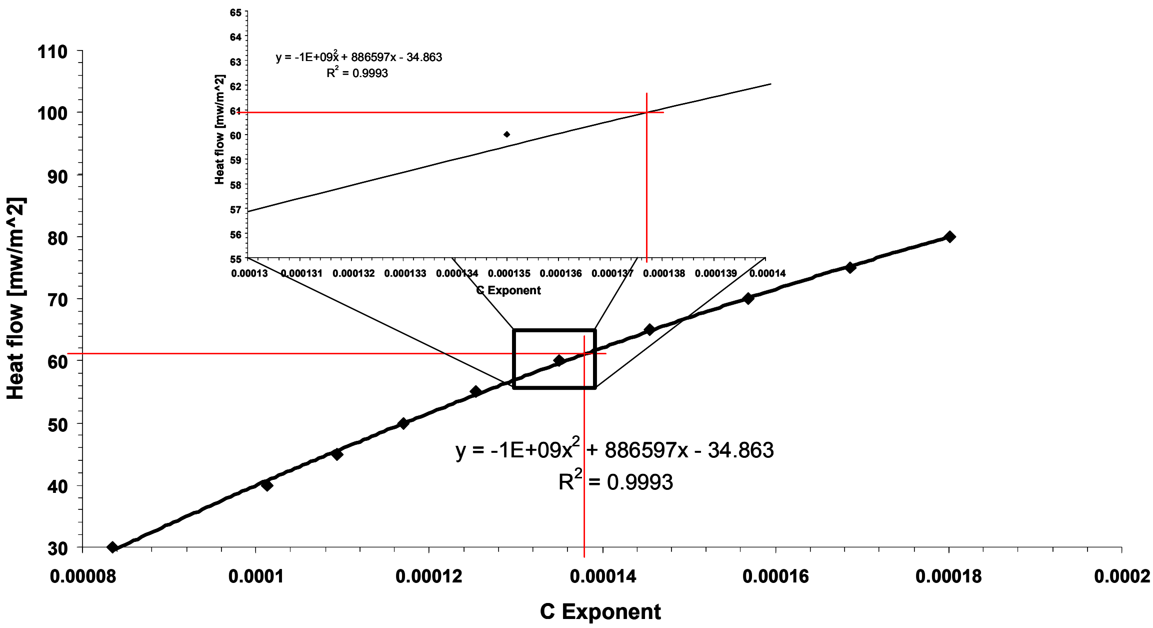

Figure 4.3: Mapping of the c exponent related to the lowest calculated MSR value versus the respective heat flow values. A function representing the continuous correlation between the two parameters is fit through the points.

Both graphs in Figure 4.2 show a less steep flank towards lower c exponents or heat flow values and a relatively steep flank towards higher c exponents or heat flow values applied to the model. This behaviour reflects the exponential effect of both the simple model equation and the complex maturity calculation method by Sweeney and Burnham (1990). In other words changes to higher c exponents or heat flow values will much quicker result in greater mismatch between the observed data and the calculated trends than changes to lower c exponents or heat flow values.

A cross plot of the respective MSR values for every calculation step within the simple and the complex model (Figure 4.4) gives evidence to validate the simple model of Thomsen and Noeth (2001) and shows the very similar, almost one-to-one behaviour of the two systems after mapping the simple into the complex.

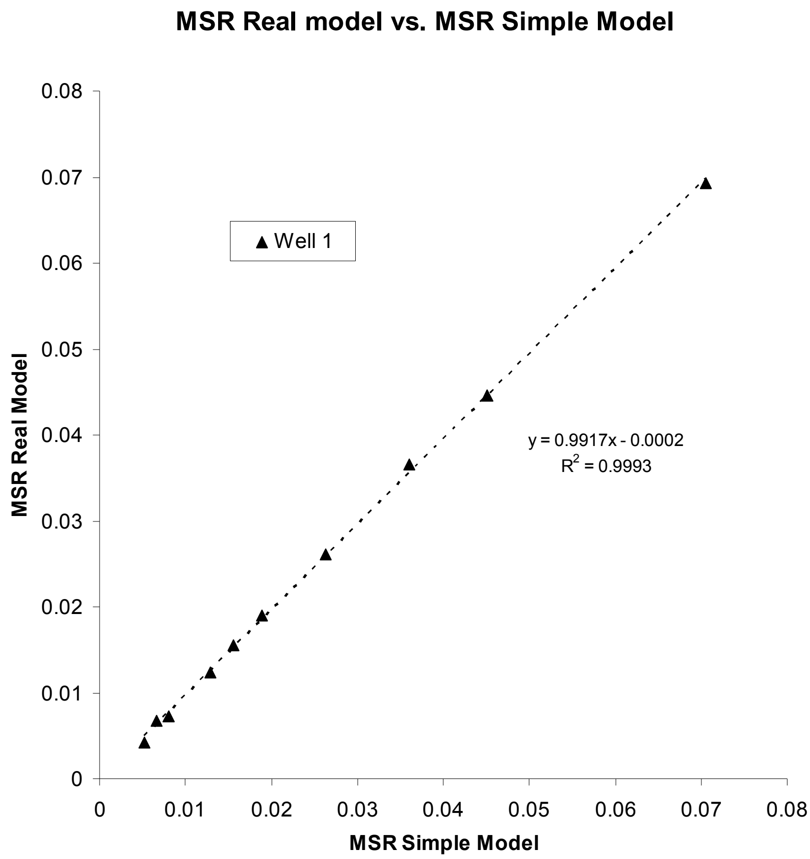

Figure 4.4: Cross plot of the MSR calculated for the simple model compared to the observed data versus the MSR calculated for the complex model compared to the measured data. The points indicate the amount of misfit at ten different heat flow values and their respective c exponents after back mapping the simple into the complex model.

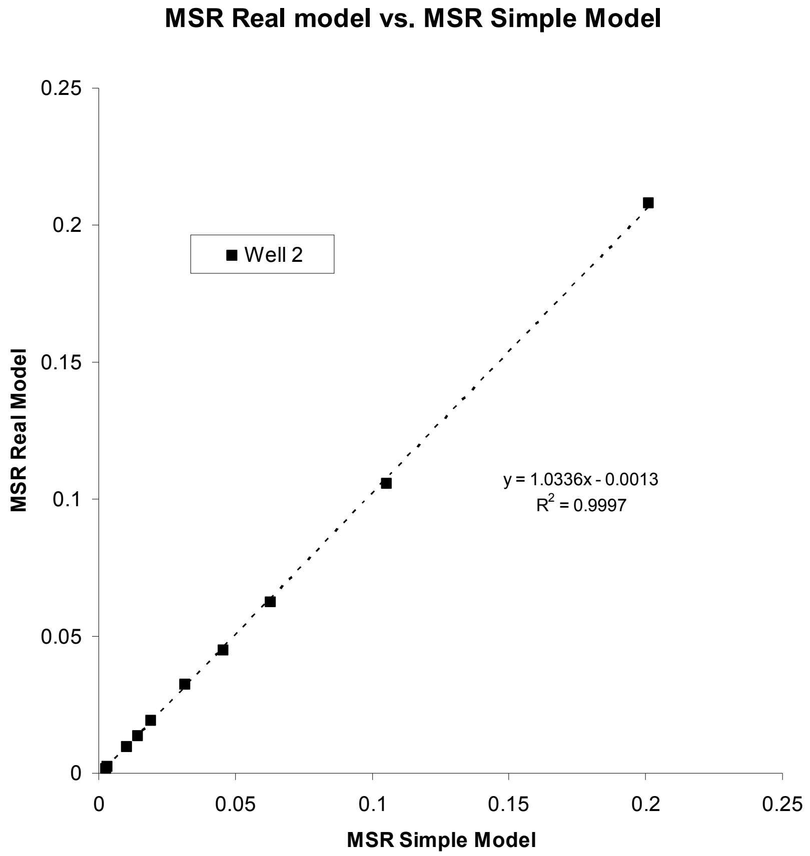

Figure 4.4: Continued.

4.4.3 Well 2

Vitrinite reflectance data available for well 2 is shown in figure 4.1. Calculations for well 2 show similar results when applying the workflow described for well 1. Different absolute values for the MSR calculations originate from "better data fit" of the measured points compared to the predicted models in well 1. The determined "best fit" heat flow of 57.6 mW/m^2 is also quiet different to the "best fit" value encountered in well 1 (61 mW/m^2). This results again from a significantly different distribution of measured data points in the well.

Nevertheless the MSR calculations and results (figure 4.4) for well 2 input parameters also verify the simple model of Thomsen and Noeth (2001) and support the assumption that the simple model reacts in the same way the complex calculation does and variation of the input parameter, heat flow or c exponent, gives the same amount of mismatch between observed data and calculated trend lines in both modelling systems.

The results for the behaviour of the two different maturity prediction approaches from both wells justify the implementation of the “Instant Sensitivity Analysis Tool”. This instrument allows a quick and graphically demonstrative determination of a lower and an upper acceptable trend line for maturity prediction in the simple model in order to quantify the uncertainty within the parameter investigated. Back mapping of the obtained c exponents to the real model gives the respective heat flow values that should be applied to the complex calculation within the basin modelling software.

4.5 Instant Sensitivity Analysis Tool

For a quick and easy evaluation of upper and lower acceptable ranges for heat flow values an “Instant Sensitivity Analysis Tool” has been developed. The setup for this tool is done within minutes in any spreadsheet software. Only five columns for input parameters are necessary to get a quick overview chart.

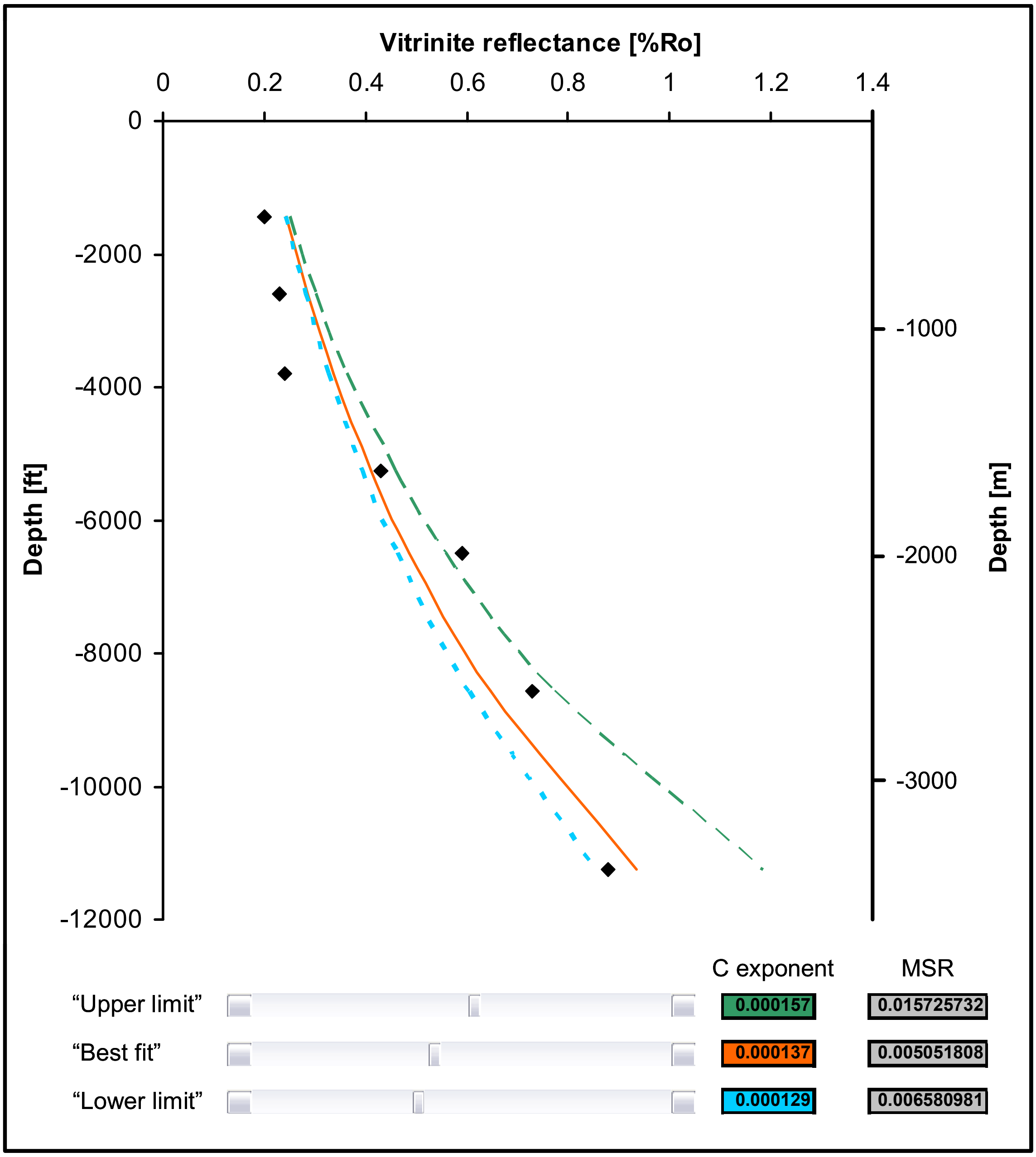

Figure 4.5: Graphic result of the “Instant Sensitivity Analysis Tool”. The figure shows an example of a possible build-up of this calibration instrument.

Column one contains the depth, column two contains the measured vitrinite reflectance data, the three last columns show results from the simple model calculation at “best fit”, “lower limit” and “upper limit”. Figure 4.5 shows the graphic results of the tool.

The three columns that contain results from the simple equation are linked to scroll bars which control the c exponent of the simple equation. One changes the input parameter for the “upper limit”, one for the “best fit” and one for the “lower limit”. The limits of the scroll bars are arbitrarily set to a minimum of 0.00005 and a maximum of 0.00025, varying in 0.000001 steps. The accuracy can of course be adjusted to personal requirements. The graphic result of the calculations is shown as a continuous line for the “best fit” case on Figure 4.5 and reacts instantly to changes in the c exponent. By dragging the scroll bars the basin modeller has a very quick graphical and also mathematical overview of the behaviour of the simple model and, as shown earlier in this article, consequently the behaviour of the complex “real” model results derived from basin modelling software calculations. The c exponents applied to the simple model calculations on Figure 4.5 are shown in the coloured boxes next to the scroll bars. Instant MSR calculations in the grey boxes behind the respective scroll bars and c exponent cells on Figure 4.5 give a quick indication of the amount of misfit of the measured data compared to the calculated trends.

Consequent back mapping of the obtained boundary c exponents in the real model gives heat flow values to use in the complex maturity calculation. No additional plot needs to be created for this purpose. Figure 4.3 shows the c exponents for well 1 at which the lowest MSR of the arbitrary basin modelling software runs were encountered plotted against the respective heat flow values. The heat flow values for the “upper” and “lower” boundary are found in this plot following the workflow for finding the “best fit” heat flow.

4.6 Conclusion

The main focus of the presented article was to verify the simple model for maturity prediction introduced by Thomsen and Noeth (2001). A cross plot of calculated misfit (expressed by the MSR) between observed data and calculated trends shows that the simple model reacts very similar to the complex model when changing the parameter investigated, in this case heat flow or c exponent. A consequent result of this study was the introduction of the “Instant Sensitivity Analysis Tool”. This instrument allows the basin modeller to predict acceptable boundaries for “lower” and “upper” acceptable trend lines calculated from the simple model describing the observed data. For calculations in the basin modelling software the c exponents obtained need to be translated into heat flow values. The limits of course will be best guesses from individuals and object for further discussions when assessing risks to the modelling study. However, the misfit of the calculated trends compared to the observed data is a measurable factor and can be monitored during the entire calibration process. Empirical calibration processes will have to be conducted in order to establish the relationship between acceptable misfit and the risk associated in the constant heat flow.

The easy and quick process of finding a “best fit” constant heat flow history does not substitute a subsequent model run in a professional basin modelling tool. Especially information on hydrocarbon generation and expulsion is derived from very complex kinetics describing the transformation process from kerogen to hydrocarbons. Those processes are very much dependent on detailed information on temperature distribution in the basin at any time. The easy model can not provide this kind of information. It is only meant to give a first indication of how the heat flow history potentially looks like when no other thermal indicator than vitrinite reflectance was observed in the basin.

5 Final Conclusions

Initial starting point of the thesis work was the investigation of the thermal history of the Horn Graben. Measurements on vitrinites have been conducted in order to receive information on the grade of maturity of the sediments the particles were found in. Its amount of reflectance is assumed to strongly correlate with the thermal maturity. An expected pattern of measured points was found for both exploration wells drilled in this area. The consequent investigation and determination of the heat flow history ended with two possible heat flow scenarios for the Horn Graben history. One history contained only one heat anomaly at the very beginning of the modelled section in Triassic times. A second heat event was added to the second probable heat flow history during the Middle Jurassic due to information from literature. Both possibilities resulted in a very similar predicted maturation trend. The hydrocarbon generation history and the transformation ratio through time looked very different though. The second heat event in the thermal history obviously had a tremendous impact on the hydrocarbon potential of the Horn Graben area. Concluding the following questions arose:

1) What justifies the implementation of this second heat event if it does not have an obvious impact on the observed maturity indicator, vitrinite reflectance?
2) What are we actually able to read out of the vitrinite reflectance data and how well resolved are the predicted maturity trends in the observations?

The first study obviously showed that the investigation of temperature history within a basin system controlled by basal heat flow is not always very obvious and many variations within heat flow histories will end with a very similar calculated and equally acceptable maturity trend. Overestimation in being able to find complex heat flow histories in sedimentary basins with calibrating to vitrinite reflectance and excessive confidence in the precise calculation of computing tools seem to lead to complicated heat flow histories which can not be justified by measured data.

A simple method for pseudo-inverse calculations introduced by Thomsen and Noeth (2001) appeared most promising to help answering the posed questions in the first part of this study. A simple equation trying to predict maturity eases the mathematical approach of finding the simplest way to model the observed data. Only a limited number of model runs within the basin modelling software are necessary for a “back map” procedure for finding the “best fit” parameter for the complex calculation equivalent to the very quickly determined parameter in the simple model. Mean Squared Residual (MSR) calculations for various settings of the parameter investigated allow finding a mathematically approved “best fit” constant heat flow value with which a “best fit” predicted maturity trend can be calculated.

Many basin modelling studies end at a point at which the basin modeller achieved a “best visual fit” of the calculated maturity trend compared to the measured vitrinite reflectance data. Additional to the very subjective way of solving the problem, this process is very time consuming due to the numerous model runs within the basin modelling software.

The second part of this thesis shows that it may not in all cases be appropriate to use a constant heat flow history to model the observed vitrinite reflectance pattern. In the case of the two Horn Graben wells, for example additional temperature data were available from the bore holes. The present day temperature field could not be represented well by applying the constant heat flow determined with the simple model. In both cases the calculated present day geothermal gradient was much higher than observed. Consequently the present day heat flow needed adjustment. Therefore another MSR calculation process was conducted in order to determine a heat flow that matches the observed temperature data from the two bore holes. The result showed expectedly that in both cases lower but very similar present day heat flow values led to “best fit” scenarios.

The results also clearly indicated that the basin must have been exposed to a heat event in the past because now the predicted maturity trends did no longer fit the observed vitrinite data using the determined “best fit” present day heat flow constantly for the modeled time. Again the easiest heat flow history was object of the investigation. A high heat flow value at the model start gradually declining to the present day “best fit” heat flow would be the easiest solution. In the subsequent MSR calculations the magnitude of the initial heat flow value was obtained. A third step was the investigation of the time at which the difference between the initially high heat flow and the lower heat flow at present day was halved. The calculation showed that the heat flow value sought is located directly on the gradually declining heat flow history already determined. No improvement of the misfit between calculated and measured data was obtained.

Sensitivity analyses and quick estimates of “best fit” and “upper” and “lower” constant heat flow values when calibrating basin models to vitrinite reflectance data is possible by using the “Instant Sensitivity Analysis Tool” introduced in the third part of the thesis. First, the behavior of the simple model compared to the behavior of the complex model was investigated in order to justify sensitivity analyses and uncertainty range investigations performed on basis of the simple maturity model. An almost linear relation between the two different approaches shows that predicted maturity from the simple model will give the same misfit of calculated data compared to measured data like the complex model. Now, only a limited number of model runs in the basin modelling software are necessary in order to obtain “best fit”, “lower” and “upper” heat flow values associated with the observed data. The instant calculation of the misfit between predicted and observed data allows a quantification of the risk in the determined heat flow histories. Overall the tool will help carrying out reproducible basin modelling studies free from very personal “visual best fit” maturity trend determinations of the basin modeller in charge.

6 Outlook

The observations of this thesis will hopefully contribute to a more reliable interpretation of what information on heat flow history is contained in the pattern of vitrinite reflectance plotted versus depth. A detailed understanding of the behavior of predicted maturity trends with changing heat flows is important especially when information on hydrocarbon generation and migration processes are claimed from a petroleum systems model. Changes of magnitude and timing of heat events in the heat flow history normally have a severe impact on the generation and expulsion of hydrocarbons even though no differences are visible in the predicted vitrinite reflectance pattern. Unless detailed information on heat events in the past is provided by other sources, no complicated heat flow history is justified through the observed vitrinite reflectance data.

The described and introduced methods help finding reproducible “best fit” model results and facilitate quantifying acceptable uncertainty ranges for the parameter investigated. An implementation in professional basin modelling software would supply avoiding overestimations in resolving predicted maturity trends in observed data.

During the process of exploring new hydrocarbon reservoirs several uncertainties in the technical work are assessed and quantified. Besides reservoir presence and quality, seal quality and trap formation the petroleum charge and timing are key factors when assessing the risk of a potential hydrocarbon reservoir. In most basin models the burial history is well defined and hence the heat flow history is the main uncertainty when quantifying processes in basin models which are related to temperature evolution through time. A “best fit” heat flow history as a mode and the distance to the “upper” and “lower” acceptable limits provide an indication of the amount of uncertainty in this parameter used for the basin modelling study. A small difference would be equivalent to a small risk. Subsequently the risk can be expressed in a percentage. The exact relation between the amount of uncertainty and the risk percentage needs further empirical calibration.

At present the decision of the risk is often derived from a personal point of view. The “Instant Sensitivity Analysis Tool” provides a very quick method of assessing the uncertainty in the heat flow history when a constant heat flow value is appropriate. Consequently the associated risk within this parameter used for modelling would be more precise and reproducible. Furthermore the process of determining the “best fit” and the “upper” and “lower” acceptable range is extensively shortened.

A first attempt to include more detailed information on the thermal distribution in sedimentary basins is included in this thesis with calculating the “best fit” temperature gradient at present day based on bore hole temperature data. In future complementary time and work need to be spent on the development of a simple model for predicting recent heat flows and geothermal gradients based on fit with measured present-day temperature data. This would help to improve and ease the pseudo-inverse calculation in those cases applying a constant heat flow history to the model is not appropriate due to additional temperature data. More detailed information on how to construct “best fit” heat flow histories could be gained from the combination of the two simple models.

7 References

Allen PA and Allen JR (1990) Basin analysis: principles and applications. Oxford

Andsbjerg J, Nielsen LH, Johannessen PN and Dybkjær K (2001) Divergent development of two neighbouring basins following the Jurassic North Sea doming event: the Danish Central Graben and the Norwegian-Danish Basin. In Martinsen OJ and Dreyer t (eds) Sedimentary environments offshore Norway-Palaeozoic to Recent. Norwegian Petroleum Society (NPF) Special Publication 10: 175-197

Beha A, Thomsen RO and Littke R (2007) Thermal history, hydrocarbon generation and migration in the Horn Graben in the Danish North Sea – a 2D basin modelling study. International Journal of Earth Sciences DOI 10.1007/s00531-007-0247-2

Berggren WA, Kent DV, Swisher CC and Aubry MP (1995) A revised Cenozoic geochronology and chronostratigraphy, In Berggren WA, Kent DV, Aubry MP and Hardenbol J (eds) Geochronology, Time Scales and Global Stratigraphic Correlation. SEPM Special Publication 54: 129-212

Best G, Kockel F and Schöneich H (1983) Geological history of the southern Horn Graben. In Kaasschieter JPH and. Reijers TJA (eds) Petroleum geology of the southeastern North Sea and the adjacent onshore areas (The Hague, 1982). Geol Mijnbouw 62: 025-033

Bethke CM (1985) A numerical model of compaction-driven groundwater flow and heat transfer and its application to paleohydrology of intracratonic sedimentary basins. Journal of Geophysical Research 90: 6817-6828

Clausen OR and Korstgård JA (1993) Faults and faulting in the Horn Graben area, Danish North Sea. First Break 11(4): 127-143

Clausen OR and Korstgård JA (1994) Displacement geometries along graben bounding faults in the Horn Graben, offshore Denmark. First Break 12(6): 305-315

Clausen OR and Korstgård JA (1996) Planar detaching faults in the southern Horn Graben, Danish North Sea. Marine and Petroleum Geology 13(5): 537-548

Doré AG, Augustson JH, Hermanrud C, Stewart DJ and Sylta Ø (eds) (1993) Basin modelling: Advances and Applications. Elsevier, 694 p

Espitalié J, Deroo G, and Marquis F (1985) La pyrolyse rock-eval et ses applications. Revue de l'Institute Francaise du Petrole 40(6): 755-785

Gradstein FM, Agterberg FP, Ogg JG, Hardenbohl J, van Veen P, Thierry J and Huang Z (1994) A Mesozoic timescale. J Geophys Res 99: 24051-24074

Hertle M and Littke R (2000) Coalification pattern and thermal modelling of the Permo-Carboniferous Saar Basin (SW-Germany). International Journal of Coal Geology 42: 273-296

Huvaz O, Karahanoglu N and Ediger V (2007) The thermal gradient history of the Thrace Basin, NW Turkey: Correlation with basin evolution processes. Journal of Petroleum Geology 30(1): 3-24

Lerche I (1988) Inversion of multiple thermal indicators: Quantitative methods of determining paleoheat flux and geological parameters. I. Theoretical development for paleoheat flux. Mathematical Geology 20: 1-36

Lerche I (1990a) Basin Analysis: Quantitative Methods, Vol. 1. Academic Press, San Diego, CA

Lerche I (1990b) Basin Analysis: Quantitative Methods, Vol. 2. Academic Press, San Diego, CA

Lerche I (1991) Inversion of dynamical indicators in quantitative basin analysis models: Theoretical Considerations. Mathematical Geology 20: 817-832

Littke R and Leythaeuser D (1993) Migration of oil and gas in coals. In Law BE and Rice DD (eds) Hydrocarbons from Coal. Amer Assoc Petr Geol, Studies in Geology 38: 219-236

Littke R, Büker C, Hertle M, Karg H, Stroetmann-Heinen V and Oncken O (2000) Heat flow evolution, subsidence, and erosion in the Rhenohercynian orogenic wedge of central Europe. In: Franke W, Haak V, Oncken O and Tanner D (eds) Orogenic processes; quantification and modelling in the Variscan Belt. Geological Society, London, Special Publications 179: 231-255

McKenzie DP (1978) Some remarks on the development of sedimentary basins. Earth planet Sci Letters 40: 25-32

Michelsen O (1989) Revision of the Jurassic Lithostratigraphy of the Danish subbasin DGU Serie_A No 24, 21 p

Nakayama K and Lerche I (1987) Basin analysis by model simulation: Effects of geologic parameters on 1D and 2D fluid flow systems with application to an oil field. Trans Gulf Coast Assoc Geol Soc 37: 175-184

Nakayama K and Van Siclen DC (1981) Simulation model for petroleum exploration. AAPG Bull 39: 1230-1255

Neunzert GH, Gaupp R and Littke R (1996) Absenkungs- und Temperaturgeschichte paläozoischer und mesozoischer Formationen im Nordwestdeutschen Becken. Z dt geol Ges 147(2): 183-208

Nielsen L, Klinkby L and Balling N (1998) Seismic evidence for deep Palaeozoic sedimentary units in the Ringkøbing-Fyn High offshore Denmark. Bulletin of the Geological Society of Denmark, Copenhagen 45: 1-10

Nielsen LH (2003) Late Triassic-Jurassic development of the Danish Basin and Fennoscandian Border Zone, southern Scandinavia. In Ineson JR and Surlyk F (eds) The Jurassic of Denmark and Greenland. Geological Survey of Denmark and Greenland Bulletin 1: 459-526

Nielsen SB (1996) Sensitivity analysis in thermal and maturity modelling. Marine and Petroleum Geology 13(4): 415-425

Noeth S, Thomsen RO and Littke R (2002) A method for assessing statistical significance and uncertainties for calibration of 1-D thermal basin maturation models. AAPG Bulletin 86(3): 417-431

Pepper AS and Corvi PJ (1995) Simple kinetic models of petroleum formation. Part I: oil and gas generation from kerogen. Marine and Petroleum Geology 12(3): 291-319

Rodon S and Littke R (2005) Thermal maturity in the Central European Basin system (Schleswig-Holstein area): results of 1D basin modelling and new maturity maps. Int J Earth Sci (Geol Rundsch) 94: 815-833

Scheck M, Thybo H, Lassen A, Abramovitz T and Laigle M (2002) Basement structure in the southern North Sea, offshore Denmark, based on seismic interpretation. In Winchester JA, Pharaoh TC and Verniers J (eds) Palaeozoic Amalgamation of Central Europe. Geological Society, London, Special Publications 201: 311-326

Scheidt and Littke (1989) Comparative organic petrology of interlayered sandstones, siltstones, mudstones and coals in the Upper Carboniferous Ruhr basin, northwest Germany, and their thermal history and methane generation. Geologische Rundschau 78: 375-390

Schoenherr J, Urai JL, Kukla PA, Littke R, Schléder Z, Larroque JM, Newall MJ, Al-Abry N, Al-Siyabi HA, Rawahi Z (in press 2007) Limits to the sealing capacity of halite: A case study of the Infra-Cambrain Ara Salt from the South Oman Salt Basin. AAPG Bulletin.

Schwarzer D and Littke R (2007) Petroleum generation and migration in the 'Tight Gas' area of the German Rotliegend natural gas play: a basin modelling study. Petroleum Geoscience 13: 37-62

Sweeney JJ and Burnham AK (1990) Evaluation of a simple model of vitrinite reflectance based on chemical kinetics. AAPG Bulletin 74(10): 1559-1570

Taylor GH, Teichmüller M, Davis A, Diessel CFK, Littke R and Robert P (1998) Organic Petrology, Stuttgart. 704 p

Thomsen RO (1994) Dynamical models in geology: Sensitivity analysis and scientific risk. Energy Exploration and Exploitation 11: 329-356

Thomsen RO (1998) Aspects of Applied Basin Modelling: Sensitivity Analysis and scientific risk. In: J. Iliffe and S. Düppenbecker (eds): Basin modelling, Practice and Progress. Geological Society of London, Special Publications, London, UK, 141: 209-221

Thomsen RO and Noeth S (2001) Uncertainties and sensitivity analysis of thermal parameters: pseudo-inversion applied to 1D forward deterministic models. Energy Exploration & Exploitation 19(4): 387-395

Tissot BP, Pelet R and Ungerer P (1987) Thermal history of sedimentary basins, maturation indices, and kinetics of oil and gas generation. American Association of Petroleum Geologists Bulletin 71: 1445-1466

Underhill JR and Partington MA (1993) Jurassic thermal doming and deflation in the North Sea: implications of the sequence stratigraphic evidence. In Parker JR (ed) Petroleum geology of Northwest Europe: Proceedings of the 4th conference: The Geological Society of London, London: 337-345

Ungerer P, Burrus J, Doligez B, Chénet PY and Bessis F (1990) Basin evaluation by integrated two-dimensional modelling of heat transfer, fluid flow, hydrocarbon generation, and migration. American Association of Petroleum Geologists Bulletin 74: 309-33

Vejbæk OV (1990) The Horn Graben, and its relationship to the Oslo Graben and the Danish Basin. In Neumann E-R (ed) Rift zones in the continental crust of Europe – geophysical, geological and geochemical evidence: Oslo-Horn Graben. Tectonophysics 178: 29-49

Waples DW (1998) Basin modelling: how well have we done? In: Düppenbecker SJ and Iliffe JE (eds): Basin modelling: Practice and Progress. Geological Society, London, Special Publications 141: 1-14

Welte DH and Yükler MA (1981) Petroleum Origin and Accumulation in Basin evolution – a quantitative Model. AAPG Bulletin 65: 1387-1397

Welte DH and Yalcin MN (1987) Basin Modelling – a new comprehensive method in petroleum geology. Org Geochem 13: 141-151

Welte DH, Horsfield B and Baker DR (eds) (1997) Petroleum and Basin Evolution. Springer Verlag, Berlin, 535 p

Yalcin MN, Littke R and Sachsenhofer RF (1997) Thermal history of sedimentary basins. In: Welte DH, Horsfield B and Baker DR (eds): Petroleum and Basin Evolution, 169-229, Springer Verlag, Berlin

Yükler MA, Cornford C and Welte DH (1978) One dimensional model to simulate geologic, hydrodynamic and thermodynamic development of a sedimentary basin. Geol Rundsch 67: 960-979

Ziegler PA (1990) Geological Atlas of Western and Central Europe. 2nd edn, Shell International Petroleum Maatschappij B.V.; Den Haag

Curriculum Vitae

Andreas Beha	Geburtstag:	06.03.1976
	Geburtsort:	Stuttgart

1995	Abitur, Gymnasium Kenzingen
08/1995 – 09/1996	Zivildienst Landvolkshochschule St. Ulrich
10/1996 – 10/1997	Universität Stuttgart: Maschinenbau
10/1997 – 12/2004	Universität Freiburg im Breisgau: Geologie
12/2004	Diplom in Geologie
04/2005 – 12/2006	Wissenschaftlicher Angestellter am Lehrstuhl für Geologie, Geochemie und Lagerstätten des Erdöls und der Kohle, RWTH Aachen
Seit 01/2007	Geologe bei Maersk Oil, Kopenhagen, Dänemark